Evolution of an acetylcholinesterase gene complex and its contribution to organophosphate insensitivity in an invasive mite pest

Joshua A Thia[1,*], Paul A Umina[1,2], Ary A Hoffmann[1]

[1] Bio21 Institute, School of BioSciences, The University of Melbourne, Melbourne, Victoria 3052, Australia

[2] Cesar Australia, Brunswick, Victoria 3056, Australia

ORCID:

Joshua A. Thia https://orcid.org/0000-0001-9084-0959

Paul A. Umina https://orcid.org/0000-0002-1835-3571

Ary A. Hoffmann https://orcid.org/0000-0001-9497-7645

Running title: *Ace* amplification in a mite pest

Keywords: agricultural pests, Australia, copy number variation, non-convergent evolution, genome scans, pesticide resistance, pool-seq, target-site mutations

Abstract

Pesticide resistance provides an intriguing system to study adaptative evolution because the candidate genes, the targets of pesticidal compounds, are often known a priori. In the redlegged earth mite, *Halotydeus destructor* (Trombidiformes: Penthaleidae, Tucker 1925), amplification of the acetylcholinesterase gene (*ace*), has led to the evolution of a gene complex. This gene complex has likely evolved in response to decades of organophosphate selection to control this invasive mite pest in the Australian grain and pasture industry. Using a pool-seq approach and experimental selection of *H. destructor* mites, we find that this *ace* gene complex likely contributes to organophosphate insensitivity in several ways. Firstly, we found that an increased copy number of individual *ace* genes within this complex is associated with organophosphate insensitivity. This effect may be general (increased copy number across all *ace* genes) or related to specific *ace* genes (the ancestral *ace* gene, HDE_14279, in a subset of populations). Secondly, target-site mutations (G119S, A201S, and F331Y) in the ancestral *ace* gene appear to be associated with evolved resistance to high doses of organophosphates. Thirdly, despite the low within-gene polymorphism, there were high levels among-gene polymorphisms at codons typically associated with resistance in other arthropods. These included fixed amino acids known to confer resistance (*e.g.,* at codons 119, 201, 227, 331, and 441), but the functional effect of these mutations at amplified *ace* genes is yet to be characterised. Although we tested for the effects of other (non-*ace*) genes (*e.g.,* detoxification on cuticular genes), our genome scans were equivocal and could not identify any other clear candidate genes contributing to organophosphate insensitivity. Our study makes headway on unravelling the intricacies of the *ace* gene complex in *H. destructor* and its phenotypic effects. We highlight the role of gene amplifications in adaptive evolution and its potential to generate polygenic-like mechanisms and non-convergent responses to selection among populations.

Introduction

Pesticide resistance in arthropod pests (insects and mites) has been extensively studied to understand the genetic basis of adaptation to toxins. Many pesticides exert their toxicity through very specific structural interactions with a target protein (*e.g.,* Russell *et al.*, 2004; Davies *et al.*, 2007; Crossthwaite *et al.*, 2014). Such precise biomolecular interactions commonly produce convergent evolution of the same mutations in the target gene ('target-site mutations') that confer pesticide resistance (Foster *et al.*, 1996; Martinez-Torres *et al.*, 1997; Khajehali *et al.*, 2010). This observed convergence in target-site mutations is striking because it occurs across diverse taxonomic levels. For example, the target gene of organophosphate pesticides is the enzyme acetylcholinesterase (*ace*), which is responsible for breaking down to acetylcholine in the synapse (Russell *et al.*, 2004). Organophosphorus pesticides inhibit this action by competitively binding to *ace*, preventing acetylcholine breakdown, leading to uncontrolled firing at the synapse and ultimately death (Oakeshott *et al.*, 2005). Many arthropod pests have evolved the same mutations that disrupt inhibition of *ace* by organophosphates, a convergence on the exact same genetic mechanism underpinning resistance (reviewed in: Fournier, 2005; Feyereisen *et al.*, 2015).

However, the genetic basis of pesticide resistance can be more complex than mutational changes in target sites. Duplications of target genes can contribute to resistance by increasing gene dosage, elevating the number of target protein molecules that must be inhibited by a pesticide to achieve mortality (Kwon *et al.*, 2010a, 2012b). Target gene duplications can also propagate haplotypes carrying target-site mutations in the

genome, increasing the proportion of target protein molecules carrying pesticide resistance mutations (Kwon *et al.*, 2010a; Carvalho *et al.*, 2012). Any fitness costs associated with the reduced catalytic activity of target-site mutations can be ameliorated by duplications. This may involve locking in heterozygote copies of gene in the same haplotype, where one susceptible copy maintains high functionality to balance the reduced functionality but resistant second copy (Alout *et al.*, 2009). Alternatively, increased expression of duplicated target genes may be beneficial because a comparable level of enzymatic activity is retained despite reduced functionality of resistant proteins (Kwon *et al.*, 2012b).

Other genes unrelated to target sites can also contribute to pesticide resistance. Well studied cases include genes involved in detoxification processes, for example, cytochrome P450s, esterases, GSTs, or ABC transporters (Devonshire & Moores, 1982; Crossley *et al.*, 2017; Walsh *et al.*, 2018). Other genes may contribute to resistance by reducing cuticle penetration by pesticides through changes in cuticle structure or composition, or by translocating pesticides more efficiently, and these genes may encode cuticular proteins, cytochrome P450s, or ABC transporters (Hsu *et al.*, 2016; Crossley *et al.*, 2017). These non-target genetic factors may make large contributions to resistance phenotypes (Devonshire & Moores, 1982; Walsh *et al.*, 2018), or smaller contributions that produce a polygenic resistance phenotype (Hsu *et al.*, 2016; Crossley *et al.*, 2017).

In this study, we focus on the redlegged earth mite, *Halotydeus destructor* (Tucker 1925; Penthaleidae, Trombidiformes), an agricultural pest mite of Australian grain and pasture crops. This mite invaded the state of Western Australia from South Africa around 1917 and spread throughout the southern regions of Australia during the 1920s (Newman, 1925; reviewed by Ridsdill-Smith, 1997). It is a winter-active pest, which diapauses as eggs during the Australian summer (October–March), emerges in autumn (April–May), and typically undergoes its active life stage through to late spring (April–November) (Ridsdill-Smith, 1997). Control of this mite for many decades has been largely achieved through the application of pyrethroid and organophosphate pesticides (Umina *et al.*, 2019; Arthur *et al.*, 2021). Tolerance to pesticides was initially observed in the 1990s and early 2000s (Hoffmann *et al.*, 1997; Robinson & Hoffmann, 2000), with pyrethroid resistance first detected in field populations in 2006 (Umina, 2007) and organophosphate resistance first detected in 2014 (Umina et al. 2017).

Whilst the molecular mechanism of pyrethroid resistance in *H. destructor* has mostly been linked to target-site mutations (Edwards *et al.*, 2018; Cheng *et al.*, 2019; Yang *et al.*, 2020), the molecular mechanism of organophosphate resistance has been difficult to elucidate. The recently assembled draft genome for *H. destructor* (Thia *et al.*, 2022) revealed a large *ace* gene amplification event, which has led to the formation of an *ace* gene complex. This *ace* amplification may be the product of a long history of organophosphate selection. In that prior work, we observed clear presence/absence patterns between organophosphate resistant/susceptible populations for target-site mutations at the ancestral *ace* HDE_14279 gene: G119S, A201S, and F331Y (Thia *et al.*, 2022). However, the role of different *ace* genes in organophosphate insensitivity has not been tested. Other genetic factors (non-*ace* genes) that might be involved (e.g., detoxification or penetrance mechanisms) also remain to be thoroughly explored.

Here, we used a whole-genome pool-seq approach to investigate the genetic basis of organophosphate resistance in populations of *H. destructor* from different geographic regions of Australia. We tested the hypotheses that: (1) copy number variation in *ace* is associated with organophosphate insensitivity; (2) target-site mutations in the *ace* gene are associated with organophosphate insensitivity; and (3) other genetic factors

(non-*ace* genes) are associated with organophosphate insensitivity. Our results suggest that genes within the *ace* complex may contribute to organophosphate insensitivity through copy number variation and target-site mutation effects. We were unable to find clear evidence of additional genetic factors that might contribute toward organophosphate insensitivity through detoxification and (or) reduced penetration. Organophosphate insensitivity appears to be multifaceted and polygenic in *H. destructor* with the potential for non-convergent genetic mechanisms evolving to produce resistance.

Methods

Organophosphate insensitivity

An individual or population is typically considered 'resistant' to a pesticide when it has evolved to survive exposure to high chemical doses. In contrast, 'susceptible' individuals (or populations) are those that have not evolved resistant and are killed at doses that an otherwise 'resistant' individuals (or populations) would survive at. The dose used to define resistance is arbitrary given the ability to survive a chemical stress is a threshold trait (Roff, 1996) and relative to the dose an individual or population is exposed to. At a high exposure dose, the nomenclature 'resistant' versus 'susceptible' is intuitive but is more subjective when populations cannot survive high doses, and (or) if a low exposure dose is used. We therefore use the term 'organophosphate insensitivity' in this study as a more precise way of separating individuals exposed to different pesticide doses in specific populations. Here, individuals within populations that survive organophosphate exposure are considered 'insensitive', whereas those that were killed by exposure are considered 'sensitive'. This definition allows us to jointly consider the responses of phenotypically 'resistant' and 'susceptible' populations to different doses of organophosphates.

Biological material

Halotydeus destructor collected for this study came from industry projects surveying phenotypic resistance in the states of Western Australian and Victoria (Figure 1). All Western Australia populations (Manjimup, Tambellup, Treeton, and Yongarillup) were found to be resistant to organophosphates. Victoria populations included two from Colbinabbin, one with evolved resistance to organophosphates (herein referred to as Colbinabbin Res) and the other susceptible to organophosphates (herein referred to as Colbinabbin Sus). A third Victorian population was collected from Wantirna South and previously used to assemble the reference genome for *H. destructor* (Thia *et al.*, 2022). Although not phenotypically screened in this study, mites from Wantirna South are known to be susceptible to organophosphates (Paul Umina, personal communication).

Collections of mites from phenotypic resistance surveys were exposed to either omethoate (Western Australia populations) or dimethoate (Victoria populations), two widely used organophosphates for mite control in Australia. The Western Australian mites used in this study were exposed to either 5.8 or 8.7 mgL^{-1} omethoate; 5.8 mgL^{-1} is a standard discriminating omethoate dose for resistance in *H. destructor* that kill phenotypically susceptible mites (Arthur *et al.*, 2021). Colbinabbin Res mites were exposed to 34 mgL^{-1} of dimethoate, and Colbinabbin Sus mites were exposed to 3.4 mgL^{-1} dimethoate. These doses produce roughly 60% mortality in their respective populations, and all mites from the Colbinabbin Sus population die at 34 mgL^{-1} (Joshua Thia, personal communication). Pesticide exposures were implemented using the coated vial method (Robinson & Hoffmann, 2000; Umina, 2007; Arthur *et al.*, 2021). Briefly, mites were collected from the field and held at 4°C

before exposure to pesticide. Pesticides were prepared by diluting stock solutions of 290 gL^{-1} omethoate (Le Mat®) or 400 gL^{-1} dimethoate (ADAMA®) in distilled water with 0.01% polysorbate 80 (Tween®), and then diluted to make up the necessary doses. Pesticides were swirled in 30 mL plastic vials to coat and left to air-dry overnight. The following day, around 50 mites were placed into the vials along with a single vetch (*Vicia sativa*) leaf. After 24 h at 18°C, mites were scored as alive (insensitive) and dead (sensitive) following Hoffmann et al. (1997). These mites were then separated, placed into Eppendorf tubes with 100% ethanol and frozen at −20°C prior to molecular analysis. For some populations, we also kept samples of untreated mites that were either unexposed to pesticides (Colbinabbin Res and Colbinabbin Sus) or were exposed to a dose that imposed 0% mortality (Manjimup to 0.87 mgL^{-1} omethoate).

Pool-seq library preparation

Alive and dead mites were used to create pooled DNA extractions using a DNeasy® Blood and Tissue Kit (Qiagen, Hilden, Germany). Each DNA extraction represented a unique biological replicate comprising 10–70 mites (see Table 1). For each DNA extraction, two 150 bp paired-end whole-genome Illumina short-read libraries were constructed by Novogene (Novogene Co. Ltd, Hong Kong), which represented technical replicates of each pooled DNA extraction. Pool-seq libraries were generated for at least one pool of alive and dead mites for all populations, except Wantirna South for which we had a single untreated collection. We also produced pool-seq libraries for untreated mites from Colbinabbin Res, Colbinabbin Sus, and Manjimup.

For downstream analysis, pool-seq libraries were aggregated to different levels. For each unique DNA pool, we always aggregated replicate pool-seq libraries. In the Manjimup and Yongarillup samples, we also aggregated different DNA pools from the same population and pesticide treatment to increase the number of pooled diploid individuals. We initially extracted DNA from smaller pool sizes to increase biological replication from available mite collections. We indicate the aggregation of DNA pools from the same population and pesticide treatment in Table 1. Herein, we refer to 'samples' as sets of aggregated DNA pools. Samples were used to establish contrasts between alive and dead mites. All populations were represented by one alive–dead pair of samples, except the Colbinabbin Res and Sus populations, for which we had two independent pairs. For the Colbinabbin Res and Sus populations, we also included a pair of untreated samples. Details of sample contrasts are provided in Table 2.

Bioinformatic processing and SNP variant calling

Raw reads for each unique pool-seq library were quality trimmed using FASTP (Chen *et al.*, 2018), truncating reads to 100 bp and discarding all reads below this threshold. Trimmed reads for each pool-seq library were mapped to the *H. destructor* reference genome (GenBank GCA_022750525.1) using BOWTIE2 (Langmead & Salzberg, 2012) with a global alignment and the '--sensitive' mapping option. Mapping was limited to contigs >0.2 Mb in length. We limited mapping to these larger contigs because prior work had identified more variable, unreliable mapping to smaller contigs (Thia *et al.*, 2022). SAMTOOLS (Li *et al.*, 2009; Danecek *et al.*, 2021) was used to discard reads with mapping quality <30 and those that were found to be PCR duplicates. Variant calling was performed using FREEBAYES (Garrison & Marth, 2012) with the arguments: '--min-alternate-count 3' and '--pooled-continuous'. The FREEBAYES script, *fasta_generate_regions.py*, was used to segment the genome for variant calling in parallel. We used BCFTOOLS (Li, 2011; Danecek *et al.*, 2021) to combine VCF files from across the parallel variant calling runs. Variant filtering was performed with VCFTOOLS (Danecek *et al.*, 2011) to retain only single nucleotide polymorphisms (SNPs; no indels) with a minor allele count of 3, a minor allele frequency

of 0.01, minimum quality of 30, minimum depth of 20 reads per sample, no missing data, and to exclude SNPs from repetitive regions of the genome.

Ace protein sequence similarity

We constructed a neighbour joining tree of *ace* proteins to visualize the sequence similarities among the *ace* genes. We imported *ace* protein sequences with the packages BIOSTRINGS v2.62.0 (Pagès *et al.*, 2017). ClustalW alignment of the *H. destructor ace* protein sequences was performed with the MSA package v1.26.0 (Bodenhofer *et al.*, 2015), with the *Torpedo californica ace* gene (GenBank X03439.1) used as an outgroup. A distance matrix among protein sequences was derived using the number of amino acid differences and pairwise deletion with the APE V5.6-2 (Paradis *et al.*, 2004). The APE package to construct a neighbour joining tree from this distance matrix, with node support estimated with 500 bootstrap replicates. The R package *ggtree* v4.2 (Yu *et al.*, 2017) was used to illustrate the tree.

Ace copy number variation

We tested the hypothesis that greater *ace* copy number is associated with organophosphate insensitivity in *H. destructor*. We used mapped read depth ratios as an estimate of *ace* copy number. We compiled a single copy gene list containing the 866 reference genes verified as single copies in prior BUSCO analyses of the *H. destructor* genome (Thia *et al*., 2022) that resided on genomic contigs >0.2 Mb in length. We extracted mean read depth information for these single copy genes and 19 *ace* genes with the SAMTOOLS COVERAGE function. Read depth statistics were then imported into R v4.1.3 (R Core Team, 2022) for further analysis.

We first summarized read depth for each gene (*ace* and single copy reference genes) per sample (see Table 1) by taking the mean across all replicate pool-seq libraries nested in DNA pools, and then taking the mean of DNA pools nested in samples. We then examined variation in *ace* copy number by calculating *ace* depth ratios. Depth ratios were calculated by dividing *ace* depth by the single copy reference gene depth (866 estimates for each of the 19 *ace* genes). The mean depth ratio for each *ace* gene was taken across all estimates from the single copy reference genes. We performed a principal components analysis (PCA) to visualize variation in depth ratios across *ace* genes and among samples using R's PRCOMP function with the arguments 'scale = FALSE, center = TRUE' to obtain an ordination from covariances between *ace* genes.

Our formal hypothesis test involved fitting a mixed effects linear model:

Ace depth ratio = Survival + State|Population + *Ace* gene + Reference gene

In this model, the response '*Ace* depth ratio' is the *ace* depth ratio. 'Survival' is the survival status, a categorical fixed effect, alive or dead. We fitted the random intercepts for 'Population' nested within 'State' of sample origin, and separate random intercepts for each of the *ace* genes, '*Ace* gene', and each single copy reference gene, 'Reference gene'. The model was fitted using the LME4 (Bates *et al.*, 2014) and LMERTEST (Kuznetsova *et al.*, 2017) R packages. To summarise differences in depth ratio between alive and dead mites, we calculated Δ_{surv}, the mean difference in depth ratio across *ace* genes (alive minus dead).

Ace target-site mutations

We tested the hypothesis that target-site mutations in the *ace* gene are associated with insensitivity in *H. destructor*. We searched for *ace* target-site mutations at codons defined a priori based on their demonstrated

resistance conferring effects in other arthropods: 73, 78, 82, 119, 128, 129, 150, 201, 201, 227, 280, 290, 328, 330, 331, 336, 435, and 441 (*Torpedo californica* numbering) (reviewed in: Fournier, 2005; Feyereisen *et al.*, 2015). We used our alignment of *H. destructor ace* protein sequences with *T. californica* to determine the homologous codon positions in *H. destructor*. We then identified the underlying nucleotide bases for each codon and determined whether any of our SNPs were associated with these a priori codons. We surveyed the 19 *ace* genes residing on genomic contigs >0.2 Mb in length.

For non-synonymous SNPs in the a priori target-site codons, we tested for significant differences in mutation frequency between alive and dead mites using a X^2 test of the observed read counts for the reference and alternate allele (a two-by-two contingency table). We calculated the frequency differential between treated alive and dead mites (or between untreated samples) in each sample pair (see Table 2) by subtracting the reference allele frequency of dead mites from that of alive mites (or one untreated sample from another). To further explore the distribution of amino acids across *ace* genes and populations, we examined the read alignments in a subset of pool-seq libraries. We extracted mapped reads from select libraries from Wantirna South, Colbinabbin Sus, Colbinabbin Res, and Manjimup populations using the GENOMICALIGNMENTS (Lawrence *et al.*, 2013) and BIOSTRINGS (Pagès *et al.*, 2017) R packages.

Genome scan

We tested the hypothesis that other non-*ace* genes contribute toward organophosphate insensitivity in *H. destructor*. An F_{ST} outlier approach was used to identify genomic regions with significant differentiation between treated alive and dead mites to identify differentiation potentially driven be organophosphate selection. We also performed these same tests on untreated sample pairs to infer the stochastic background differentiation expected. We aggregated pool-seq libraries to generate reference and alternate allele read counts for working sample pairs in R (Table 1). We used the POOLFSTAT R package to filter SNPs. For each working sample pair (Table 2), SNPs were filtered at a minor allele frequency threshold of 0.1. We then defined SNP blocks as genomic regions comprising 30–50 SNPs, resulting in a median SNP block size of 6,040 bp, and a range of 1,022–82,863 bp.

We first calculated estimates of F_{ST} for each SNP. We calculated SNP-wise estimates of F_{ST} 'corrected' for sample size and technical error using POOLFSTAT:

$$F_{ST} = \frac{Q_1 - Q_2}{1 - Q_2}$$

Here, Q_1 is the identity in state probability for two genes sampled within a population pool, and Q_2 is the identity in state probability for two genes sampled between two population pools. This formulation is equivalent to ϑ, as defined by Weir & Cockerham's (1984). We also calculated an 'uncorrected' F_{ST} (Weir & Cockerham, 1984):

$$F_{ST} = \frac{\sigma}{\bar{p}(1 - \bar{p})}$$

Where σ is the variance in the reference allele frequency and $\bar{p}$ is the mean reference allele frequency. After calculating SNP-wise estimates of F_{ST}, we calculated block-wise F_{ST} by diving the mean numerator by the mean denominator components for all SNPs within a block. We therefore had block-wise F_{ST} estimates corrected and uncorrected for sample size and technical error. SNP blocks exhibiting unusually high genetic differentiation

were identified using a two-step method. The uncorrected block-wise F_{ST} values were subjected to the algorithm described in the OUTFLANK method (Whitlock, 2019) to identify a set of 'preliminary' outlier blocks. To execute the OUTFLANK method, we used a hybrid script comprised of custom code and functions borrowed from the OUTFLANK GitHub (used to calculate effective degrees of freedom and the two-sided X^2 test-statistic *p* value). The preliminary outlier blocks were retained if they exceeded the 99th percentile calculated from corrected block-wise F_{ST} values. Those blocks passing both steps comprised our 'final' outlier blocks.

We identified genes residing in the final outlier blocks as candidate genes potentially contributing to organophosphate insensitivity. Gene ontology (GO) enrichment analysis was performed to test whether certain types of genes were over-represented in this candidate gene set. GO enrichment was performed for GO terms associated with candidate genes for each treated alive–dead sample pair using Fisher's exact test in R. Significant enrichment was assessed following Bonferroni correction of *p* values.

Results

Bioinformatics summary

Following trimming, our FASTQ files for individual pool-seq libraries contained a mean of 29,570,401 reads with a range of 21,791,964–41,049,660 reads. The mean number of reads mapping to the *H. destructor* genome (genomic contigs >0.2 Mb) was 15,522,450 reads with a range of 11,132,739–23,519,859 per individual pool-seq library.

Ace protein sequence similarity

The neighbour joining tree protein sequences is illustrated in Figure 2. The *ace* genes of *H. destructor* exhibit a high degree of protein dissimilarity. The number of amino acid differences ranged from 4 to 1053, with a mean of 461.5 amino acids. The magnitude of these differences is not only contributed by underlying variation in the amino acid residues, but also by variation in length of *ace* protein products. The *H. destructor ace* proteins range from 231 to 1096 amino acids long, with a mean of 559.7 amino acids. Hence, amplification of *ace* in the *H. destructor* genome has coincided with considerable evolution of coding potential and protein product size.

Ace copy number variation

We found support for our hypothesis that greater copy numbers of the *ace* gene are associated with organophosphate insensitivity, but the role of copy number may vary by *ace* gene and (or) population. Most of the *ace* genes had depth ratios that were distributed around 1.00, suggesting they existed largely as single copies (Figure 3a). However, a few *ace* genes had depth ratios that deviated notably from 1.00 in some or all samples. In *ace* HDE_14279, the ancestral *ace* gene, samples from three Western Australia populations, Manjimup, Treeton, and Yongarillup, had depth ratios ranging from 1.49–2.37. In contrast, several other *ace* genes had depth ratios <1.00 across all samples: HDE_12794 (0.55–0.86), HDE_09715 (0.16–0.50), HDE_09713 (0.36–0.64), HDE_09712 (0.53–0.82), and HDE_09711 (0.73–0.91).

PCA of depth ratios revealed two major axes that described almost all the variation (~90%) across genes and mite samples (Figure 3b). The first PC axis separated the Western Australian populations, Manjimup, Treeton, and Yongarillup, from all other populations, capturing their larger depth ratios for *ace* HDE_14279 (Figure 3b).

The second PC axis separated the alive organophosphate exposed mite samples from Colbinabbin Sus and Colbinabbin Res from their associated dead and untreated samples, and the Wantirna South and Tambellup samples (Figure 3b).

Our linear mixed effects model of *ace* depth ratio identified a highly significant fixed 'Survival' effect ($F_{1,196558}$ = 749.13, $p < 0.001$), but the overall effect was small. On average, alive mites had a depth ratio of 0.91 (±0.06 SE), whereas dead mites on average had a depth ratio of 0.89 (± 0.0007 SE, $\beta_{\text{Dead}} = -0.02$, $t = -27.37$, df = 196558, $p < 0.001$). However, for specific populations, the mean difference in depth ratio between alive and dead mites (Δ_{surv}) was not always positive (Figure 3c). For the Colbinabbin Res (0.09 ± 0.01 SE), Colbinabbin Sus (0.07 ± 0.01 SE), Treeton (0.04 ± 0.02 SE), and Yongarillup (0.09 ± 0.01 SE), Δ_{surv} was positive, indicating an overall trend for higher copy numbers in alive versus dead mites. In contrast, Manjimup (–0.05 ± 0.03 SE) and Tambellup (–0.05 ± 0.02 SE) had negative Δ_{surv}, indicating an overall trend for lower copy numbers in alive versus dead mites.

Ace target-site mutations

We did not find consistent support for our hypothesis that *ace* target-site mutations are associated with organophosphate insensitivity. However, the presence of target-site mutations at the ancestral *ace* HDE_14279 may be indicative of resistance risk in local populations. Among our 19 focal *ace* genes and 19 a priori *ace* target-sites codons surveyed, only 6 non-synonymous SNPs were identified across all samples. One SNP was observed in *ace* HDE_01555, a L331M mutation; one SNP was observed in *ace* HDE_01576, a R238K mutation; and four SNPs were observed in the ancestral *ace* HDE_14279, producing G119S, A201S, F331Y, and L336M mutations. Contrasts between alive and dead sample pairs did not return any consistent effects: no single mutation was significantly greater in alive vs. dead mites across all populations (Figure 4a). The only significant tests were for three mutations in ancestral *ace* HDE_14279: G119S (Manjimup and Tambellup), A201S (Yongarillup), and F331Y (Manjimup and Yongarillup).

Only the G119S, A201S, and F331Y mutations in the ancestral *ace* HDE_14279 were found exclusively in resistant populations of *H. destructor* (and were completely absent in susceptible populations). The Wantirna South and Colbinabbin Sus populations from Victoria were both fixed for the reference alleles G119, A201, and F331 at ancestral *ace* HDE_14279 (Figure 4b), which are the ancestral alleles and putatively susceptible. The resistant populations varied in their mutation frequencies at *ace* HDE_14279. Correlations between the three mutations at *ace* HDE_14279 suggests that different haplotypes are segregating in local populations (Figure 4b). The A201S and F331Y mutations did not (or rarely) occurred in the same resistant population: populations with the mutant allele at one of these sites were fixed (or nearly fixed) for the reference allele at the other site (Figure 4b, right panel). In contrast, the G119S mutation was negatively correlated with A201S and (or) F331Y in some populations. For Colbinabbin Res, Tambellup, and Yongarillup, as the ancestral G119 allele increased in frequency (*i.e.,* the S119 mutant allele decreased in frequency), the ancestral A201 allele decreased in frequency (*i.e.,* the S201 mutant allele increased in frequency) (Figure 4b, left panel). For Manjimup, Treeton, and Yongarillup, as the ancestral G119 allele increased in frequency (*i.e.,* the S119 mutant allele decreased in frequency), the ancestral F331 allele decreased in frequency (*i.e.,* the Y331 mutant allele increased in frequency) (Figure 4b, middle panel). In other words, the apparent observable phases for resistant mutations appear to be: G119/S201, S119/A201, G119/Y331, S119/F331.

Although there was very little within-gene level polymorphism at the 19 a priori codons, there was considerable between-gene level polymorphism (Figure 5). Across the 19 analysed *ace* genes, there was an

average of 7.1 variants (amino acids or deletions) at a priori target-site codons, with a range of 3 to 13 variants. Particularly interesting was the observation that some *ace* genes in *H. destructor* were fixed for amino acids that are known to confer resistance in other arthropods (Feyereisen *et al.*, 2015). Most striking were the following codons: codon 119, with 5/17 genes fixed for either A119 or S119 (Figure S1); codon 201, with 12/17 genes fixed for S201 (Figure S2); codon 227, with 8/18 genes fixed for A227 (Figure S3); codon 331, with 2/18 genes fixed for H331 (Figure S4); and codon 441, with 6/18 genes fixed for G441 (Figure S5). It is worth noting that some of the analysed genes did not have an equivalent codon, hence, $n \neq 19$. These unusual fixed putatively resistance conferring amino acids were found in both susceptible and resistant populations.

Genome scan

There was equivocal support for the hypothesis that other (non-*ace*) genes are associated with insensitivity to organophosphates in *H. destructor*. On average, corrected block-wise F_{ST} between sample pairs of alive and dead mites ranged from 0.008 to 0.035, with a mean of 0.0192, across the different populations. For Colbinabbin Res and Colbinabbin Sus, we had two independent untreated sample pairs that allowed us to assess the expected background corrected block-wise F_{ST}, which was 0.012 for both populations. This genetic differentiation between untreated samples was larger or equivalent to treated sample pairs (alive versus dead) in both the Colbinabbin Res and Colbinabbin Sus populations. These results suggest that any genetic differentiation resulting from selection imposed by organophosphate exposure in our treated mites is unable to be detected above a background of stochastic sampling noise in allele frequencies.

To see if any biological patterns could be observed despite the stochasticity in F_{ST} estimates, we examined the genes identified in the outlying blocks of the alive–dead sample pairs. Across these pairs, 474 unique genes were identified as potential candidates for organophosphate insensitivity. Of these candidate genes, 17 were shared by two populations, and the remaining 457 were found in single populations. There was very little evidence for significant GO term enrichment in any alive–dead sample pair after accounting for multiple testing. Of those significant GO terms, 'Mannose metabolic process' and 'alpha-mannosidase activity' were enriched in the Colbinabbin Res 'treated 2' sample pair, and 'microtubule-based process' and 'dyein complex' were enriched in the Manjimup 'treated' sample pair. None of these GO terms have clear links to pesticide resistance. Furthermore, there was only one instance where an outlier block contained an *ace* gene (HDE_01553), but this was for an untreated sample pair (Colbinabbin Sus, sample 5 vs 4) where neither sample had been exposed to organophosphates.

Discussion

This study provides evidence that a combination of copy number and target-site mutations in the *H. destructor ace* complex may contribute toward organophosphate insensitivity. The *ace* gene amplification appears widely distributed across Australia, and we recovered sequences from all 19 analysed *ace* genes in both resistant and susceptible populations. There is variation in copy number within and among *ace* genes, and among populations, which may lead to different contributions in organophosphate insensitivity. Whilst our linear model found a general positive effect of copy number on organophosphate insensitivity, not all populations exhibited an association of higher copy number in alive versus dead mites. For some populations, e.g., Manjimup, Treeton and Yongarillup, copy number at ancestral *ace* HDE_14279 may be more important than

overall copy number across *ace* genes. In these populations, *ace* HDE_14279 had the greatest copy numbers of any *ace* gene, ranging from 1.49–2.37, and had the largest differences between alive and dead mites. Because ancestral *ace* HDE_14279 is also segregating for target-site mutations, duplications of *ace* HDE_14279 may be beneficial for over-expressing resistant *ace* proteins (Alout *et al.*, 2009; Kwon *et al.*, 2012b).

Our analyses of candidate *ace* target-site codons in *H. destructor* revealed that there were very few within-gene polymorphisms that may be related to organophosphate insensitivty. Across 19 candidate target-site codons from 19 analysed *ace* genes, only six non-synonymous mutations were identified in three *ace* genes: L331M in HDE_01554; R238K in HDE_01576; G119S, A201S, F331Y, and L336M in HDE_14279. Only three of the mutations found in HDE_14279 have been reported in the literature for other arthropod pests (Khajehali *et al.*, 2010; Kwon *et al.*, 2010b; Zhang *et al.*, 2015). Furthermore, G119S, A201S or F331Y were never observed from susceptible mite populations (Colbinabbin Sus and Wantirna South), indicating these mutations are likely to contribute to organophosphate insensitivity in resistant populations. However, when comparing alive and dead mites from resistant populations, we did not find any consistent allele frequency differences between them that would indicate repeatable shifts in favour of the putatively resistant target-site mutations. Examination of allele frequency correlations between the HDE_14279 target-site resistance mutations suggests that they may be segregating on different haplotypes. If these mutations were in phase, we would expect to see a positive correlation between them (Li *et al.*, 2015), but instead, co-occurring mutations always exhibited a negative correlation. Hence, selection for one target-site mutation (haplotype) may drive down the frequency of another target-site mutation (haplotype). It is also possible that target-site mutations vary in their contributions to insensitivity, and (or) have different effects under different genetic backgrounds (Li *et al.*, 2015; Riga *et al.*, 2017), which would also contribute to variable patterns among pools of insensitive mites.

Although candidate *ace* target-sites were not very polymorphic within genes, we observed considerable among-gene polymorphism at a prior target-site codons. The diversity of amino acids in the different *ace* lineages was striking, especially considering that many of these target-sites are highly conserved across arthropods, and animals more generally (reviewed in: Fournier, 2005; Feyereisen *et al.*, 2015). This among-gene diversity has presumably been facilitated by the *ace* amplification in the *H. destructor* genome. Duplication may relax evolutionary constraints on genes, allowing them to evolve more freely (Lynch & Conery, 2000). However, we also observed a considerable number of genes that were fixed for amino acids known to confer resistance in other arthropods: A/S119, S201, A227, H331, and G441 (Baek *et al.*, 2005; Khajehali *et al.*, 2010; Kwon *et al.*, 2012a). It seems unlikely that so many genes within the *ace* complex would possess these fixed mutations purely by chance. Given the majority of these amino acids (A119, A227, H331, and G441) are not segregating in the ancestral *ace* HDE_14279, they most likely emerged during the *ace* amplification and spread throughout the genome. However, we do not know the functionality of the amplified *ace* genes in *H. destructor*. A neutral hypothesis would be that these fixed amino acids persist because the genes they occur in are no longer functional and they do not impact fitness. Indeed, these amino acids are fixed even in susceptible populations, so their contribution to organophosphate insensitivity, if any, must be small.

Our genome scans did not provide any clear signatures of additional (non-*ace*) genes that may be involved in responses to organophosphates. None of our outlier SNP blocks contained *ace* genes in contrasts between samples of alive and dead mites. Additionally, there was no evidence for enrichment of gene families expected to contribute toward pesticide insensitivity through detoxification (*e.g.,* cytochrome P450s, GSTs, esterases, or ABC transporters) or through reduced penetrance (*e.g.,* cuticular proteins) (reviewed in: Feyereisen, 2006; Feyereisen *et al.*, 2015; Thia *et al.*, 2021). However, a major limitation of our genome scans was that genetic

differentiation between organophosphate treated alive and dead mites was indistinguishable from that of mite samples that were not exposed to organophosphates. We only had untreated sample pairs for the Colbinabbin Sus and Colbinabbin Res populations. In these cases, the 99th percentile and outlier SNP blocks exhibited similar F_{ST} values between untreated and treated sample pairs. Separating biological signature from stochastic sampling variance was not possible due to our pool-seq approach. In this study, pool-seq was an attractive option because *H. destructor* are very small and challenging to extract sufficient high-quality DNA from individuals. Sampling biases in pool-seq can emerge from two levels: allelic sampling of the pooled sample, and allelic sampling of the population (Gautier *et al.*, 2013; Hivert *et al.*, 2018). Pooling at least 30 diploids can reduce allelic sampling biases *within* pooled samples (Gautier *et al.*, 2013), and we achieved this for Colbinabbin Sus and Colbinabbin Res populations (≥40 diploids). Assuming allele frequency estimation *within* samples was accurate for these populations, contrasts *between* independent untreated samples would reflect sampling bias of population allele frequencies and stochastic genetic differentiation, which is on par with any genetic differentiation due to our organophosphate selection treatments. Given the constraints on our genome scans, we cannot draw any strong conclusions about the role of genes on organophosphate insensitivity in *H. destructor*.

Based on our findings, our working hypothesis is that different *ace* genes within the *ace* complex of *H. destructor* may contribute toward organophosphate insensitivity through a combination of copy number variation and target-site mutations. Such a multifaceted organophosphate target-gene mechanism has been observed in other arthropods, for example, mosquitoes (Alout *et al.*, 2009), aphids (Shang *et al.*, 2014), and spider mites (Carvalho *et al.*, 2012). In *H. destructor*, the roles of *ace* copy number variation and target-site mutations appear to vary among populations, leading to non-convergent adaptive responses. Whilst we have been able to unravel some of the intricacies of *ace* evolution in *H. destructor*, there are still many outstanding questions. For example, how does copy number variation and allelic composition of *ace* genes jointly influence their contribution toward organophosphate insensitivity? Do *ace* target-site mutations vary in their effect and (or) fitness costs? What are the expressional and functional differences of the *ace* genes? Addressing these questions will help elucidate the importance of individual *ace* genes and the repeatability of their effects across mite populations.

Given the accelerating spread of organophosphate resistance across Australian populations of *H. destructor* (Arthur *et al.*, 2021) clear diagnostic genetic markers of resistance would be highly advantageous (Thia *et al.*, 2021).Yet several challenges will constrain the development of such markers: (i) the intricacy of the *ace* gene complex; (ii) undetermined additional genetic factors that may contribute to resistance; (iii) non-convergent and polygenic adaptive responses among population to organophosphate selection. Excluding possible contributions of other genes, variation in the *ace* gene complex alone (copy number and allelic composition) may provide multiple ways for resistance to evolve through combinations of small effect variants. The situation for organophosphate resistance differs from pyrethroid resistance in this species where target-site mutations at the *para* sodium channel can reliably predict resistance, with small contributions of background detoxification genes (Edwards *et al.*, 2018; Yang *et al.*, 2020). At present, the ancestral *ace* gene, HDE_14279, remains the strongest candidate gene for organophosphate resistance in *H. destructor*. HDE_14279 had the highest inferred copy numbers in some resistant populations and was the only *ace* gene in which susceptible populations were fixed for susceptible alleles and resistant populations were segregating for target-site mutations (G119S, A201S, and F331Y). Whilst our work has unravelled some of the intricacies of the *ace* gene

complex in *H. destructor*, there remain several exciting avenues for future genomic and experimental studies to better discern the genetic architecture of organophosphate insensitivity in this pest.

Acknowledgements

This work was funded by the Grains Research Development Corporation (Australia) as part of the Australian Grains Pest Innovation Program, and with support from the University of Melbourne. Computational resources were provided by The University of Melbourne's Research Computing Services and the Petascale Campus Initiative.

Data accessibility

All sequencing data has been submitted under the GenBank Project PRJNA756307 and their accessions are listed in Table 1. All code required to run these analyses will be deposited into a Dryad archive and made available when this manuscript has been published.

Author contributions

JT formulated the original project design. PU and AH contributed to project design and obtained funding. JT performed all analyses. JT wrote the original manuscript. PU and AH contributed toward revisions of the final manuscript.

Tables and figures

Table 1. Metadata for pool-seq libraries. All *H. destructor* libraries were nested in DNA pools nested in biological samples (NCBI SRA and BioSample accession numbers listed for each library).

Sample	Pool	Library	Population	No. diploid individuals	Pesticide	Pesticide dose (mg a.i./L)	Survival status	State [1]	Collection year	SRA	BioSample
1	1	1_1_A	Wantirna South	70	None (untreated)	0	Control	VIC	2020	SRR15698717	SAMN20863738
2	2	2_2_A	Colbinabbin Sus	50	None (untreated)	0	Control	VIC	2021	SRR20755205	SAMN30107459
2	2	2_2_B	Colbinabbin Sus	50	None (untreated)	0	Control	VIC	2021	SRR20755204	SAMN30107460
3	3	3_2_A	Colbinabbin Sus	50	None (untreated)	0	Control	VIC	2021	SRR20755193	SAMN30107461
3	3	3_2_B	Colbinabbin Sus	50	None (untreated)	0	Control	VIC	2021	SRR20755182	SAMN30107462
4	4	4_1_A	Colbinabbin Res	50	None (untreated)	0	Control	VIC	2021	SRR20755171	SAMN30107463
4	4	4_1_B	Colbinabbin Res	50	None (untreated)	0	Control	VIC	2021	SRR20755160	SAMN30107464
5	5	5_1_A	Colbinabbin Res	50	None (untreated)	0	Control	VIC	2021	SRR20755149	SAMN30107465
5	5	5_1_B	Colbinabbin Res	50	None (untreated)	0	Control	VIC	2021	SRR20755146	SAMN30107466
6	6	6_2_A	Colbinabbin Sus	40	None (untreated)	3.4	Alive	VIC	2021	SRR20755145	SAMN30107467
6	6	6_2_B	Colbinabbin Sus	40	Dimethoate	3.4	Alive	VIC	2021	SRR20755144	SAMN30107468
7	7	7_2_A	Colbinabbin Sus	40	Dimethoate	3.4	Alive	VIC	2021	SRR20755203	SAMN30107469

7	7	7_2_B	Colbinabbin Sus	40	Dimethoate	3.4	Alive	VIC	2021	SRR20755202	SAMN30107470
8	8	8_1_A	Colbinabbin Sus	50	Dimethoate	3.4	Dead	VIC	2021	SRR20755201	SAMN30107471
8	8	8_1_B	Colbinabbin Sus	50	Dimethoate	3.4	Dead	VIC	2021	SRR20755200	SAMN30107472
9	9	9_2_A	Colbinabbin Sus	50	Dimethoate	3.4	Dead	VIC	2021	SRR20755199	SAMN30107473
9	9	9_2_B	Colbinabbin Sus	50	Dimethoate	3.4	Dead	VIC	2021	SRR20755198	SAMN30107474
10	10	10_2_A	Colbinabbin Res	40	Dimethoate	34	Alive	VIC	2021	SRR20755197	SAMN30107475
10	10	10_2_B	Colbinabbin Res	40	Dimethoate	34	Alive	VIC	2021	SRR20755196	SAMN30107476
11	11	11_2_A	Colbinabbin Res	40	Dimethoate	34	Alive	VIC	2021	SRR20755195	SAMN30107477
11	11	11_2_B	Colbinabbin Res	40	Dimethoate	34	Alive	VIC	2021	SRR20755194	SAMN30107478
12	12	12_1_A	Colbinabbin Res	50	Dimethoate	34	Dead	VIC	2021	SRR20755192	SAMN30107479
12	12	12_1_B	Colbinabbin Res	50	Dimethoate	34	Dead	VIC	2021	SRR20755191	SAMN30107480
13	13	13_1_A	Colbinabbin Res	50	Dimethoate	34	Dead	VIC	2021	SRR20755190	SAMN30107481
13	13	13_1_B	Colbinabbin Res	50	Dimethoate	34	Dead	VIC	2021	SRR20755189	SAMN30107482
18	18	18_X_A	Tambellup	20	Omethoate	5.8	Alive	WA	2019	SRR20755188	SAMN30107483
18	18	18_X_B	Tambellup	20	Omethoate	5.8	Alive	WA	2019	SRR20755187	SAMN30107484
19	19	19_1_A	Tambellup	25	Omethoate	5.8	Dead	WA	2019	SRR20755186	SAMN30107485
19	19	19_1_B	Tambellup	25	Omethoate	5.8	Dead	WA	2019	SRR20755185	SAMN30107486
20	20	20_1_A	Treeton	24	Omethoate	5.8	Alive	WA	2019	SRR20755184	SAMN30107487

20	20	20_1_B	Treeton	24	Omethoate	5.8	Alive	WA	2019	SRR20755183	SAMN30107488
21	21	21_1_A	Treeton	18	Omethoate	5.8	Dead	WA	2019	SRR20755181	SAMN30107489
21	21	21_1_B	Treeton	18	Omethoate	5.8	Dead	WA	2019	SRR20755180	SAMN30107490
26|28 [2]	26	26_2_A	Yongarillup	14	Omethoate	5.8	Alive	WA	2019	SRR20755179	SAMN30107491
26|28 [2]	26	26_2_B	Yongarillup	14	Omethoate	5.8	Alive	WA	2019	SRR20755178	SAMN30107492
26|28 [2]	28	28_2_A	Yongarillup	25	Omethoate	5.8	Alive	WA	2019	SRR20755175	SAMN30107495
26|28 [2]	28	28_2_B	Yongarillup	25	Omethoate	5.8	Alive	WA	2019	SRR20755174	SAMN30107496
27|29 [2]	27	27_2_A	Yongarillup	29	Omethoate	5.8	Dead	WA	2019	SRR20755177	SAMN30107493
27|29 [2]	27	27_2_B	Yongarillup	29	Omethoate	5.8	Dead	WA	2019	SRR20755176	SAMN30107494
27|29 [2]	29	29_2_A	Yongarillup	14	Omethoate	5.8	Dead	WA	2019	SRR20755173	SAMN30107497
27|29 [2]	29	29_2_B	Yongarillup	14	Omethoate	5.8	Dead	WA	2019	SRR20755172	SAMN30107498
32|33 [2]	32	32_X_A	Manjimup	12	Omethoate	0.87	Control	WA	2019	SRR20755170	SAMN30107499
32|33 [2]	32	32_X_B	Manjimup	12	Omethoate	0.87	Control	WA	2019	SRR20755169	SAMN30107500
32|33 [2]	33	33_1_A	Manjimup	10	Omethoate	0.87	Control	WA	2019	SRR20755168	SAMN30107501
32|33 [2]	33	33_1_B	Manjimup	10	Omethoate	0.87	Control	WA	2019	SRR20755167	SAMN30107502
38|39 [2]	38	38_X_A	Manjimup	15	Omethoate	8.7	Alive	WA	2019	SRR20755157	SAMN30107511
38|39 [2]	38	38_X_B	Manjimup	15	Omethoate	8.7	Alive	WA	2019	SRR20755156	SAMN30107512
38|39 [2]	39	39_1_A	Manjimup	15	Omethoate	8.7	Alive	WA	2019	SRR20755155	SAMN30107513
38|39 [2]	39	39_1_B	Manjimup	15	Omethoate	8.7	Alive	WA	2019	SRR20755154	SAMN30107514
40|41 [2]	40	40_1_A	Manjimup	12	Omethoate	8.7	Dead	WA	2019	SRR20755153	SAMN30107515
40|41 [2]	40	40_1_B	Manjimup	12	Omethoate	8.7	Dead	WA	2019	SRR20755152	SAMN30107516
40|41 [2]	41	41_X_A	Manjimup	12	Omethoate	8.7	Dead	WA	2019	SRR20755151	SAMN30107517
40|41 [2]	41	41_X_B	Manjimup	12	Omethoate	8.7	Dead	WA	2019	SRR20755150	SAMN30107518

[1] VIC = Victoria; WA = Western Australia

[2] In the Manjimup and Yongarillup samples, we aggregated different DNA pools from the same population and pesticide treatment to increase the number of pooled diploid individuals

Table 2. Sample contrasts for testing genetic differences between pooled *H. destructor* samples that were untreated (stochastic background differences) or treated (potential selected differences) with organophosphate.

Sample 1	Sample 2	Code	Population	Contrast
2	3	ColS: untreated	Colbinabbin Sus	Untreated
4	5	ColR: untreated	Colbinabbin Res	Untreated
6	8	ColS: treated 1	Colbinabbin Sus	Treated
7	9	ColS: treated 2	Colbinabbin Sus	Treated
10	12	ColR: treated 1	Colbinabbin Res	Treated
11	13	ColR: treated 2	Colbinabbin Res	Treated
18	19	Tamb: treated	Tambellup	Treated
20	21	Tree: treated	Treeton	Treated
26|28	27|29	Yong: treated	Yongarillup	Treated
38|39	40|41	Manj: treated	Manjimup	Treated

Table 3. Single Nucleotide Polymorphisms (SNPs) within candidate *ace* target-site codons and their effects on coding potential in *H. destructor*. The ancestral *ace* gene (HDE_14279) is bolded.

Tcal	Hdes	*Ace* gene ID number	Contig	Position	Ref allele	Alt allele	Non-synonymous
78	86	HDE_01576	utg155	546035	V (GTA)	V (GTG)	.
119	129	HDE_09762	utg48	258743	G (GGG)	G (GGA)	.
	191	**HDE_14279**	**utg94**	**20925**	**G (GGC)**	**S (AGC)**	**Yes**
128	277	HDE_13905	utg83	1999982	E (GAG)	E (GAA)	.
150	159	HDE_01556	utg155	503437	P (CCC)	P (CCA)	.
201	210	HDE_01553	utg155	499445	S (TCG)	S (TCT)	.
	207	HDE_05340	utg31	94639	S (TCA)	S (TCG)	.
201	**272**	**HDE_14279**	**utg94**	**21168**	**A (GCC)**	**S (TCC)**	**Yes**
227	337	HDE_01190	utg153	521028	G (GGC)	G (GGA)	.
	5	HDE_01555	utg155	501653	A (GCG)	A (GCA)	.
227	238	HDE_02989	utg19	1187910	G (GGA)	G (GGC)	.
238	241	HDE_01576	utg155	546499	R (AGG)	K (AAG)	Yes
331	97	HDE_01555	utg155	501929	L (CTC)	M (CTG)	Yes
	326	HDE_01576	utg155	546755	H (CAC)	H (CAT)	.
	401	**HDE_14279**	**utg94**	**21556**	**F (TTC)**	**Y (TAC)**	**Yes**
336	450	HDE_01190	utg153	521367	F (TTT)	F (TTC)	.
	406	**HDE_14279**	**utg94**	**21572**	**L (CTA)**	**M (CTG)**	**Yes**
396	544	HDE_07881	utg40	396829	G (GGC)	G (GGT)	.
441	589	HDE_07881	utg40	396694	G (GGC)	G (GGA)	.

Note: Codons are reported with respect to their candidate *ace* position in *T. californica* ('Tcal') and their relative *H. destructor* codon ('Hdes'). Alleles are reported with respect to their amino acid residue, with nucleotide bases comprising the codon in brackets.

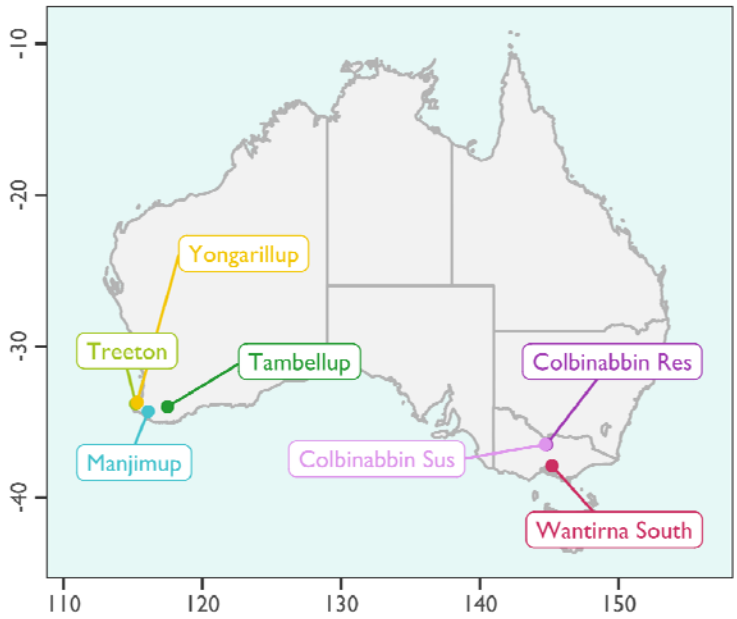

Figure 1. Map of Australia illustrating the locations of our studied populations

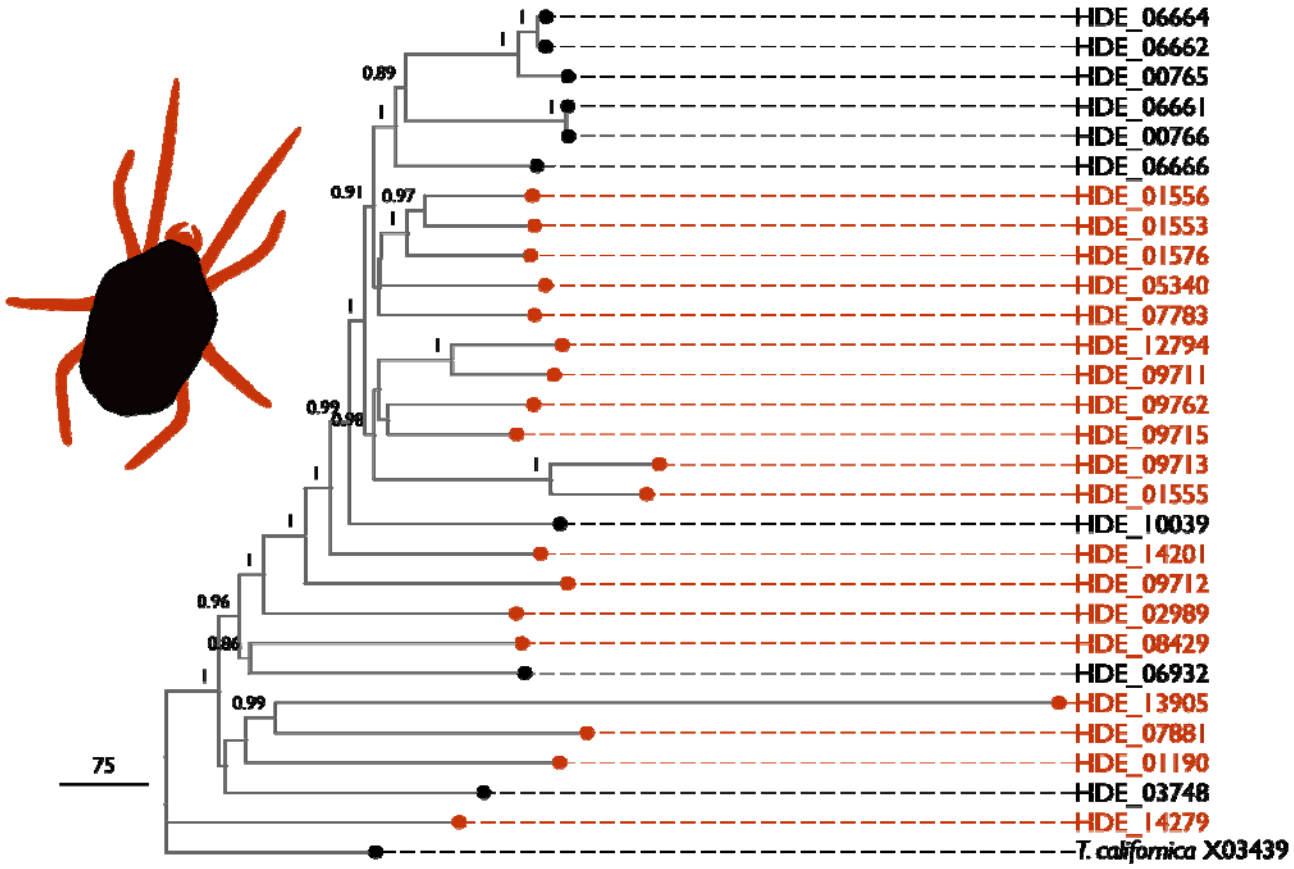

Figure 2. Neighbour joining tree of *H. destructor ace* genes (protein sequences), rooted on the *Torpedo californica ace* gene. The scale bar depicts the number of amino acid differences. *Ace* genes coloured red are those that reside on contigs >0.2 Mb in length and were analysed in this study. A cartoon illustration of *H. destructor* sits to the left of the tree.

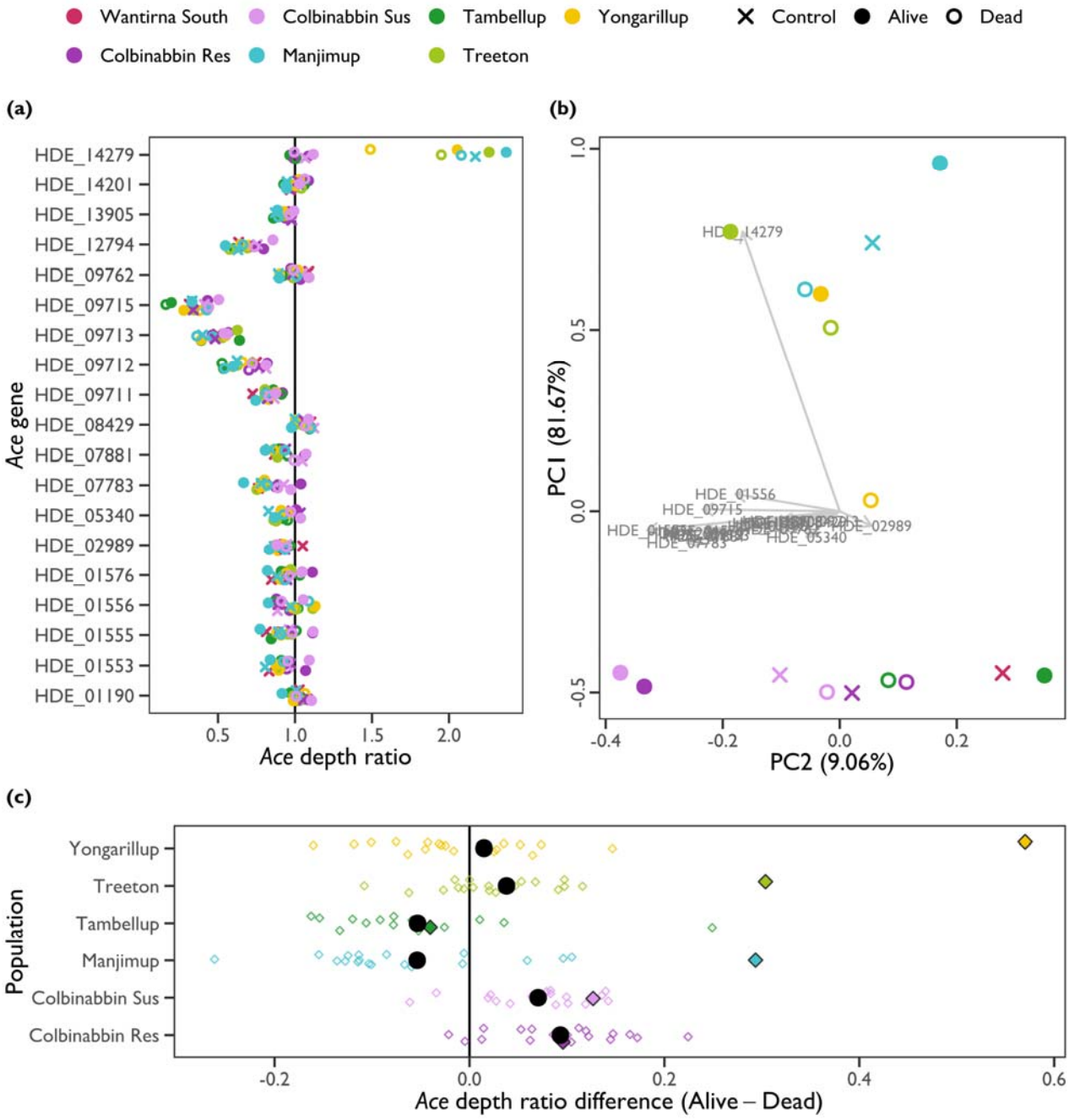

Figure 3. *Ace* depth ratios (a proxy for copy number) in pool-seq samples of *H. destructor*. (a) Mean depth ratio across 19 analysed *ace* genes. The *x*-axis is the mean depth ratio across 866 single copy reference genes and the *y*-axis is the *ace* genes. Points represent samples: colors and shapes denote population and survival status. The vertical line demarcates a difference of zero. (b) Scatterplot of the leading two PC axes summarizing variation in *ace* depth ratios *ace* genes and mite samples. The *y*-axis is the first PC axes, and the *x*-axis is the second PC axes, with the percent of total explained variance in parentheses in the axis titles. Points represent samples: colors and shapes denote population and survival status. Grey arrows depict the relative loadings of each *ace* gene to the ordination, with gene IDs on the arrow heads. (c) Difference in *ace* depth ratios between alive and dead mites within different mite populations. The *x*-axis is the mean *ace* depth ratio of alive mites minus that of dead mites, and the *y*-axis is the populations. The large coloured diamonds (with dark edge)

depict the ancestral *ace* HDE_14279, and smaller coloured diamonds depict the remaining 18 analysed *ace* genes. The large circles represent the means across all *ace* genes. The vertical line demarcates a difference of zero.

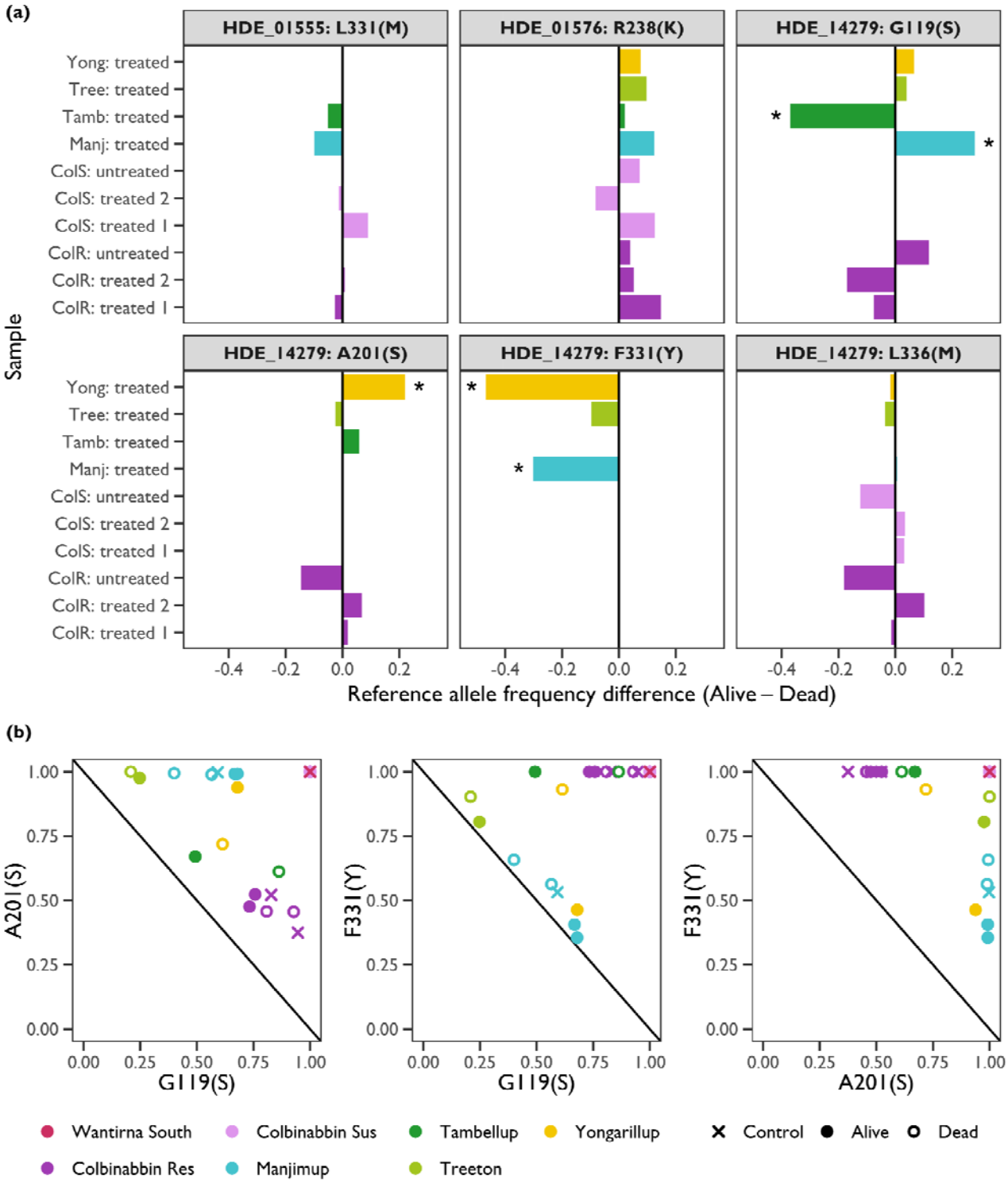

Figure 4. Allelic variation at non-synonymous mutations at candidate *ace* target-sites codons in *H. destructor* (with *Torpedo californica* numbering). (a) Reference allele frequency difference between alive and dead samples ('test') or between two control samples ('control'). Bars on the *x*-axis represents the allele frequency difference, coloured by population. Negative values indicate samples of alive mites had lower reference allele frequencies (higher alternative allele frequencies) relative to samples of dead mites. The asterisks denote significant allele count differences following Bonferroni correction for multiple tests (χ^2 test, α = 0.05/50 =

0.001). Samples are on *y*-axis, with population codes are: 'ColR' = Colbinabbin Res, 'ColS' = Colbinabbin Sus, 'Manj' = Manjimup, 'Tamb' = Tambellup, 'Tree' = Treeton, and 'Yong' = Yongarillup. Each panel represents an *ace* gene, the candidate target-site codon and reference allele, with the alternate allele in parentheses. (b) Reference allele frequency correlations for candidate *ace* target-site mutations at the ancestral *ace* gene HDE_14279. The *x*-axis and *y*-axis represent one of three *ace* target-site codons, labelled with the respective codon and reference (putatively susceptible) allele, with the alternate (putatively resistant) allele in parentheses. Increasing values on both axes represent an increasing frequency of the reference allele, whereas decreasing values on both axes represent an increasing frequency of the alternate allele. The 1:1 negative correlation is depicted by the black line. Symbols represent samples, with colours denoting population, and shapes denoting survival group.

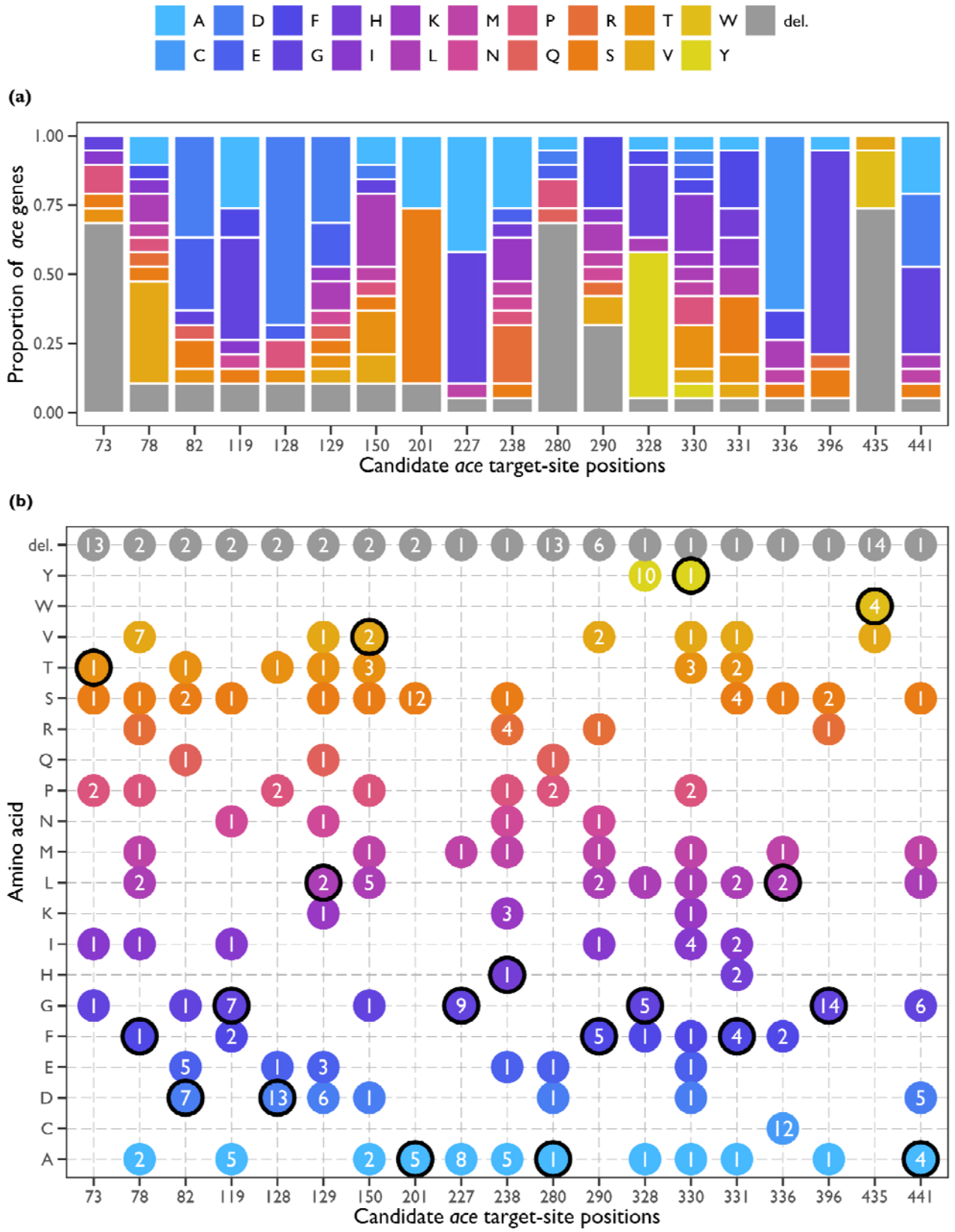

Figure 5. Reference amino acids for 19 analysed *H. destructor ace* genes (on contigs >200 Mb) at candidate target-site codons (*T. californica* numbering). (a) Amino acid proportions. The *x*-axis is the candidate *ace* target-

site codon, the *y*-axis is the relative proportion of *ace* genes exhibiting a particular amino acid as their reference allele in the *H. destructor* genome. Bars are coloured relative to amino acid. (b) Amino acid counts. The *x*-axis is the candidate *ace* target-site codon, the *y*-axis is the *ace* gene numbers exhibiting a particular amino acid as their reference allele in the *H. destructor* genome. A black outline denotes the amino acid present in the ancestral *ace* gene, HDE_14279. (a, b) 'del.' indicates a deletion, that is, there is not an equivalent codon in the *H. destructor ace* gene relative to *T. californica*.

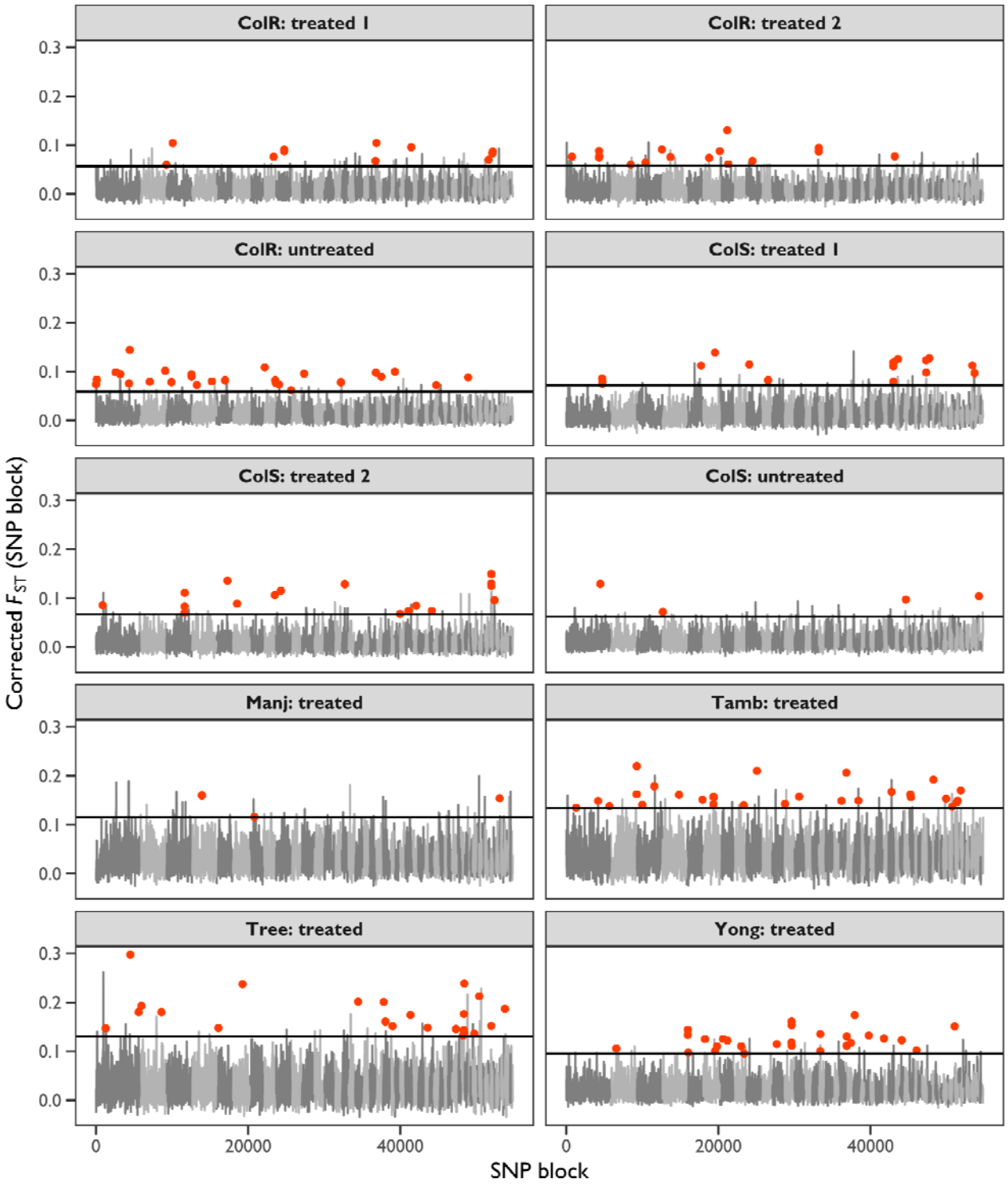

Figure 6. Genome scans of genetically differentiated genomic regions between samples of *H. destructor*. The *x*-axis represents the SNP block, indexed by contig size and linear order. The *y*-axis represents the genetic differentiation between samples, F_{ST} corrected for sampling variance. The black horizontal lines demarcate the 99th percentile of the F_{ST} value. Grey lines track the F_{ST} of *non-outlier* SNP blocks, with alternating shades of grey delimiting separate contigs. Red points denote *outlier* SNP blocks. Panels contain different sample contrasts (see Table 2). Population codes are as follows: 'ColR' = Colbinabbin Res, 'ColS' = Colbinabbin Sus,

‘Manj’ = Manjimup, ‘Tamb’ = Tambellup, ‘Tree’ = Treeton, and ‘Yong’ = Yongarillup. Sample contrasts include ‘untreated’, which is the F_{ST} between two samples *unexposed* to organophosphate, and ‘treated’, which is the F_{ST} between samples of alive and dead mites that were *exposed* to organophosphate.

Supplementary information

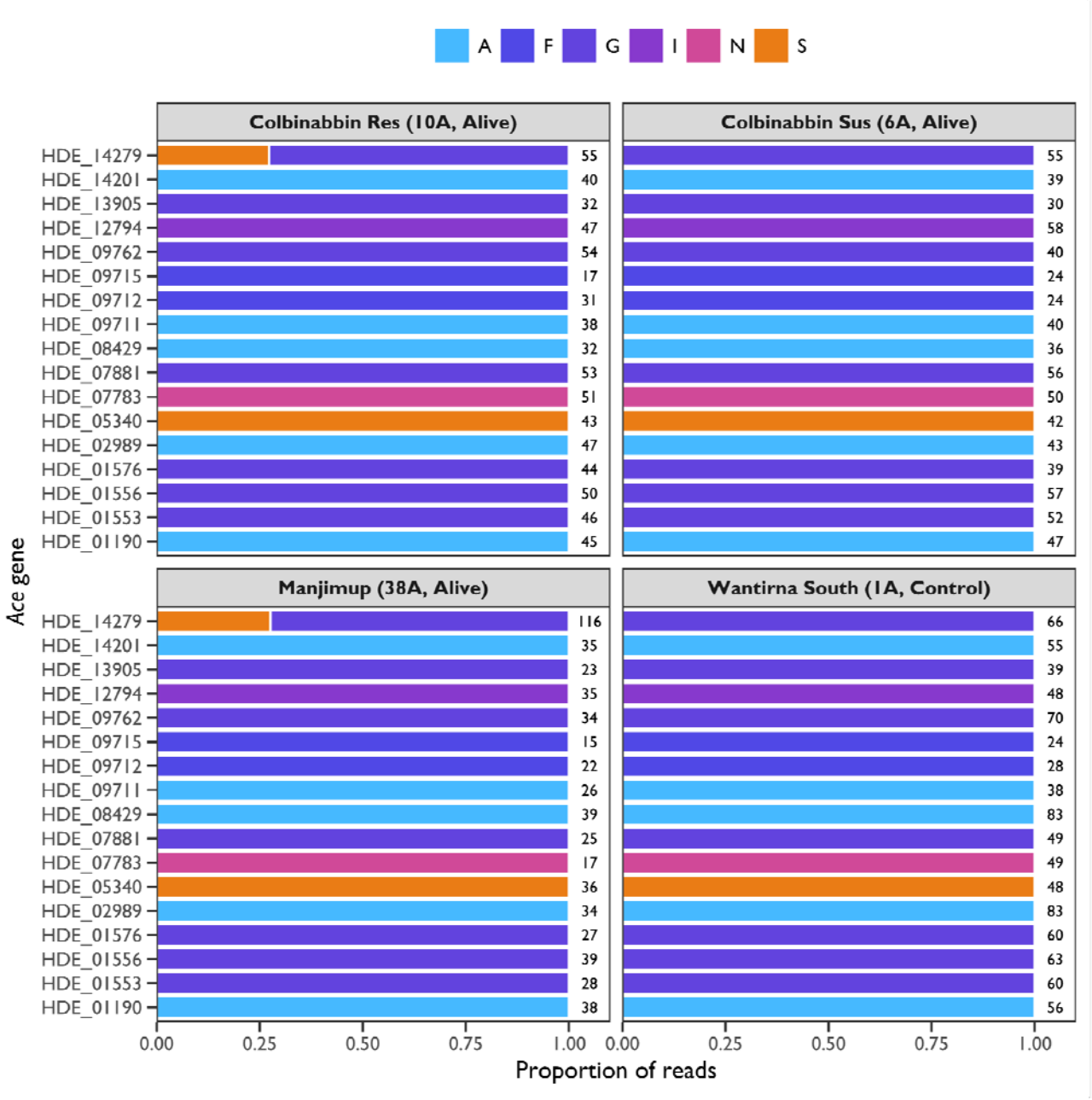

Figure S1. Proportion of reads for different amino acids at codon 119 (*Torpedo californica* numbering) across *ace* genes in *Halotydeus destructor*. The *x*-axis is the proportion of reads and the *y*-axis the *ace* gene. Horizontal bars represent the proportion of reads with nucleotide sequences encoding different amino acids, see legend. Numbers to the right of the bars indicate the number of observed reads that completely covered the codon. Panels contain observations for select pool-seq libraries, read as 'Population (DNA pool, Survival group)'. Note, Colbinabbin Res and Manjimup are resistant to organophosphates, whereas Colbinabbin Sus and Wantirna South are susceptible.

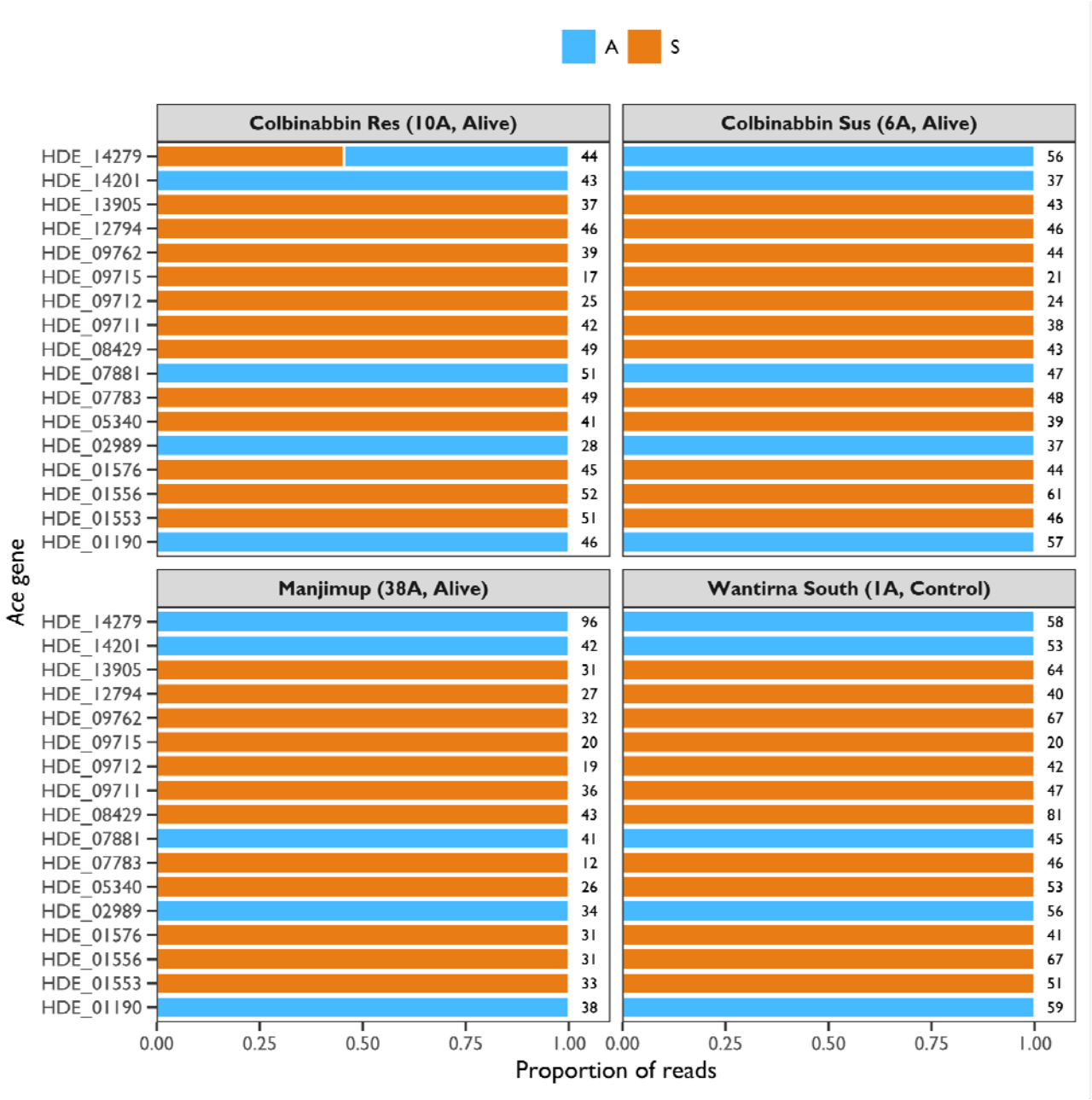

Figure S2. Proportion of reads for different amino acids at codon 201 (*Torpedo californica* numbering) across *ace* genes in *Halotydeus destructor*. The *x*-axis is the proportion of reads and the *y*-axis the *ace* gene. Horizontal bars represent the proportion of reads with nucleotide sequences encoding different amino acids, see legend. Numbers to the right of the bars indicate the number of observed reads that completely covered the codon. Panels contain observations for select pool-seq libraries, read as 'Population (DNA pool, Survival group)'. Note, Colbinabbin Res and Manjimup are resistant to organophosphates, whereas Colbinabbin Sus and Wantirna South are susceptible.

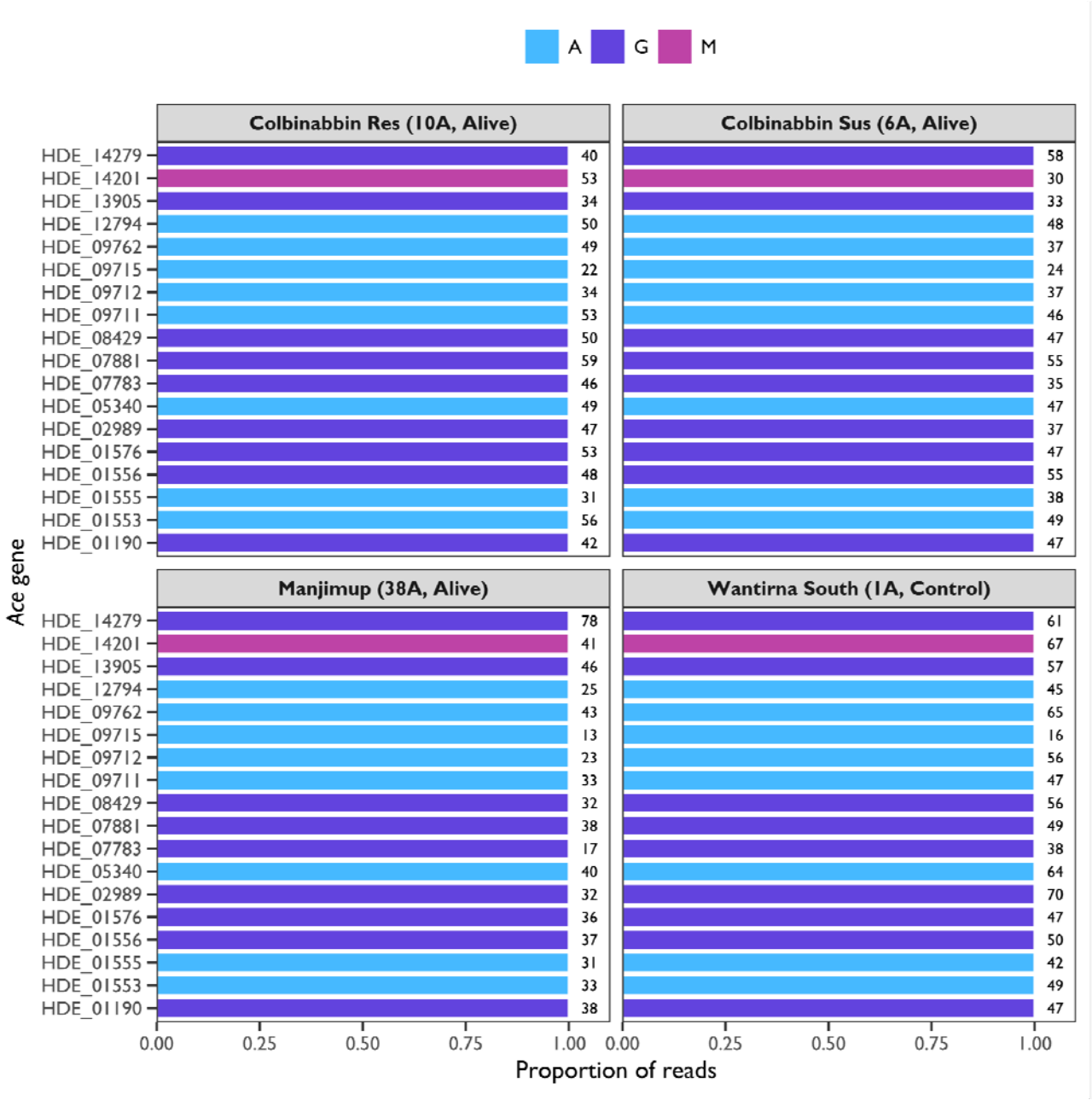

Figure S3. Proportion of reads for different amino acids at codon 227 (*Torpedo californica* numbering) across *ace* genes in *Halotydeus destructor*. The *x*-axis is the proportion of reads and the *y*-axis the *ace* gene. Horizontal bars represent the proportion of reads with nucleotide sequences encoding different amino acids, see legend. Numbers to the right of the bars indicate the number of observed reads that completely covered the codon. Panels contain observations for select pool-seq libraries, read as 'Population (DNA pool, Survival group)'. Note, Colbinabbin Res and Manjimup are resistant to organophosphates, whereas Colbinabbin Sus and Wantirna South are susceptible.

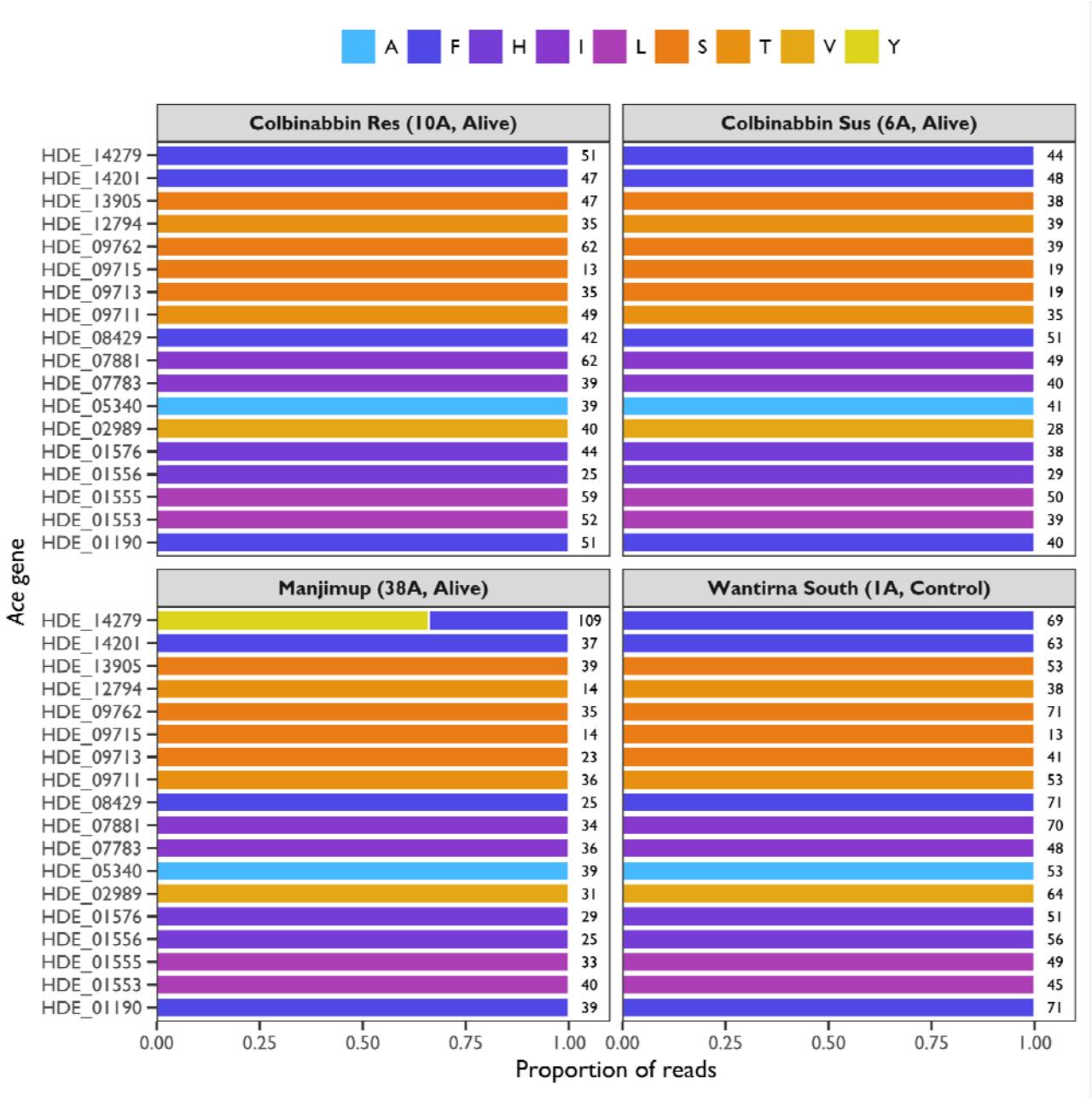

Figure S4. Proportion of reads for different amino acids at codon 331 (*Torpedo californica* numbering) across *ace* genes in *Halotydeus destructor*. The *x*-axis is the proportion of reads and the *y*-axis the *ace* gene. Horizontal bars represent the proportion of reads with nucleotide sequences encoding different amino acids, see legend. Numbers to the right of the bars indicate the number of observed reads that completely covered the codon. Panels contain observations for select pool-seq libraries, read as 'Population (DNA pool, Survival group)'. Note, Colbinabbin Res and Manjimup are resistant to organophosphates, whereas Colbinabbin Sus and Wantirna South are susceptible.

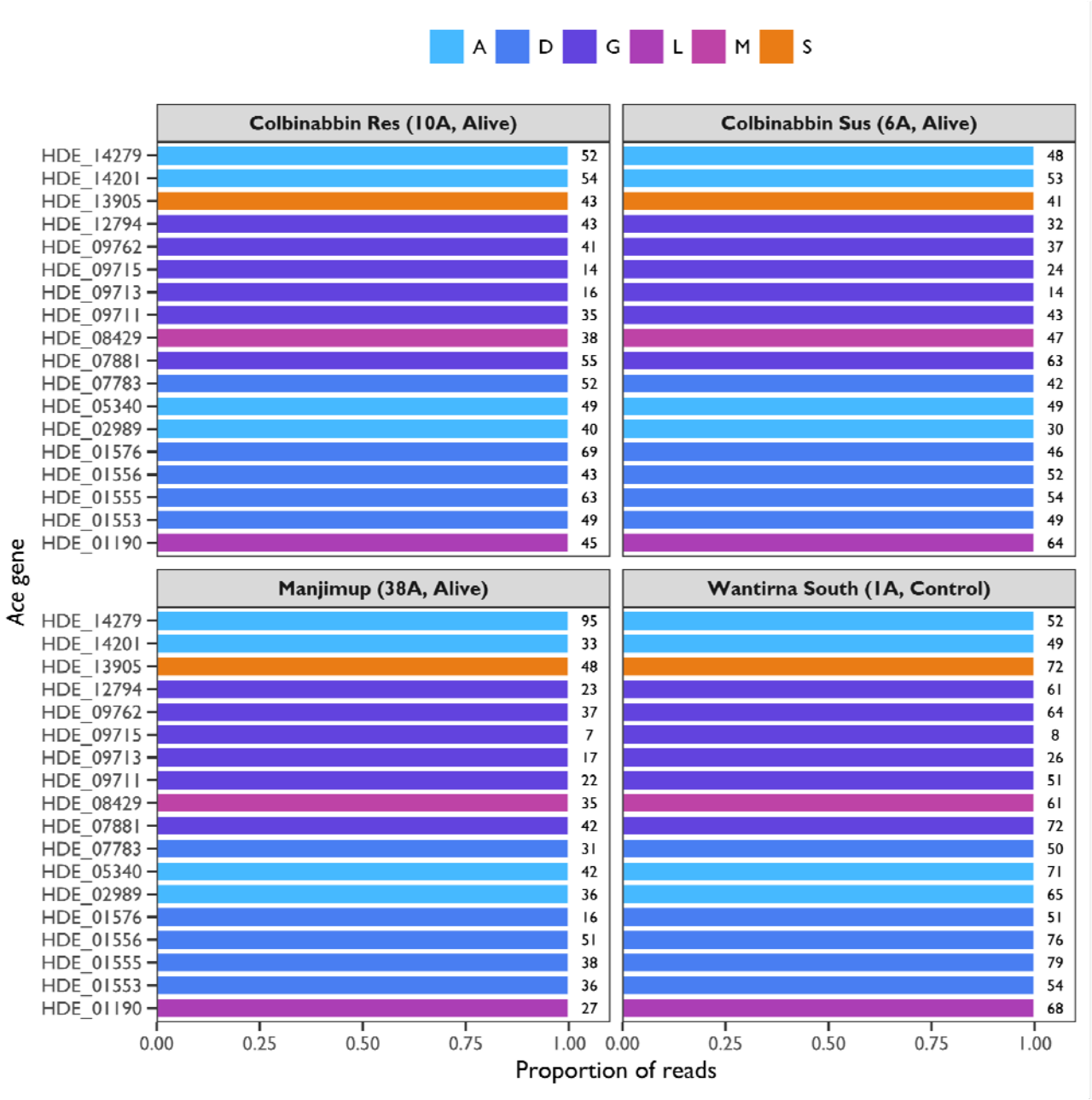

Figure S5. Proportion of reads for different amino acids at codon 441 (*Torpedo californica* numbering) across *ace* genes in *Halotydeus destructor*. The *x*-axis is the proportion of reads and the *y*-axis the *ace* gene. Horizontal bars represent the proportion of reads with nucleotide sequences encoding different amino acids, see legend. Numbers to the right of the bars indicate the number of observed reads that completely covered the codon. Panels contain observations for select pool-seq libraries, read as 'Population (DNA pool, Survival group)'. Note, Colbinabbin Res and Manjimup are resistant to organophosphates, whereas Colbinabbin Sus and Wantirna South are susceptible.

References

Alout, H., Labbé, P., Berthomieu, A., Pasteur, N. & Weill, M. 2009. Multiple duplications of the rare ace-1 mutation F290V in *Culex pipiens* natural populations. *Insect Biochem. Mol. Biol.* **39**: 884–891.

Arthur, A.L., Maino, J., Hoffmann, A.A., Jasper, M., Lord, A., Micic, S., *et al.* 2021. Learnings from over a decade of increasing pesticide resistance in the redlegged earth mite, *Halotydeus destructor* (Tucker). *Pest Manag. Sci.* **77**: 3013–3024.

Baek, J.H., Kim, J. Il, Lee, D.W., Chung, B.K., Miyata, T. & Lee, S.H. 2005. Identification and characterization of *ace1*-type acetylcholinesterase likely associated with organophosphate resistance in *Plutella xylostella*. *Pestic. Biochem. Physiol.* **81**: 164–175.

Bates, D., Mächler, M., Bolker, B. & Walker, S. 2014. Fitting linear mixed-effects models using lme4. *arXiv Prepr.*

Bodenhofer, U., Bonatesta, E., Horejš-Kainrath, C. & Hochreiter, S. 2015. msa: an R package for multiple sequence alignment. *Bioinformatics* **31**: 3997–3999.

Carvalho, R., Yang, Y., Field, L.M., Gorman, K., Moores, G., Williamson, M.S., *et al.* 2012. Chlorpyrifos resistance is associated with mutation and amplification of the acetylcholinesterase-1 gene in the tomato red spider mite, *Tetranychus evansi*. *Pestic. Biochem. Physiol.* **104**: 143–149. Elsevier Inc.

Chen, S., Zhou, Y., Chen, Y. & Gu, J. 2018. fastp: an ultra-fast all-in-one FASTQ preprocessor. *Bioinformatics* **34**: i884–i890.

Cheng, X., Umina, P.A., Lee, S.F. & Hoffmann, A.A. 2019. Pyrethroid resistance in the pest mite, *Halotydeus destructor*: Dominance patterns and a new method for resistance screening. *Pestic. Biochem. Physiol.* **159**: 9–16.

Crossley, M.S., Chen, Y.H., Groves, R.L. & Schoville, S.D. 2017. Landscape genomics of Colorado potato beetle provides evidence of polygenic adaptation to insecticides. *Mol. Ecol.* 6284–6300.

Crossthwaite, A.J., Rendine, S., Stenta, M. & Slater, R. 2014. Target-site resistance to neonicotinoids. *J. Chem. Biol.* **7**: 125–128.

Danecek, P., Auton, A., Abecasis, G., Albers, C.A., Banks, E., DePristo, M.A., *et al.* 2011. The variant call format and VCFtools. *Bioinformatics* **27**: 2156–2158.

Danecek, P., Bonfield, J.K., Liddle, J., Marshall, J., Ohan, V., Pollard, M.O., *et al.* 2021. Twelve years of SAMtools and BCFtools. *Gigascience* **10**: giab008. Oxford University Press.

Davies, T.G.E., Field, L.M., Usherwood, P.N.R. & Williamson, M.S. 2007. DDT, pyrethrins, pyrethroids and insect sodium channels. *IUBMB Life* **59**: 151–162.

Devonshire, A.L. & Moores, G.D. 1982. A carboxylesterase with broad substrate specificity causes organophosphorus, carbamate and pyrethroid resistance in peach-potato aphids (*Myzus persicae*). *Pestic. Biochem. Physiol.* **18**: 235–246.

Edwards, O.R., Walsh, T.K., Metcalfe, S., Tay, W.T., Hoffmann, A.A., Mangano, P., *et al.* 2018. A genomic approach to identify and monitor a novel pyrethroid resistance mutation in the redlegged earth mite, *Halotydeus destructor*. *Pestic. Biochem. Physiol.* **144**: 83–90.

Feyereisen, R. 2006. Evolution of insect P450. *Biochem. Soc. Trans.* **34**: 1252–1255.

Feyereisen, R., Dermauw, W. & Van Leeuwen, T. 2015. Genotype to phenotype, the molecular and physiological dimensions of resistance in arthropods. *Pestic. Biochem. Physiol.* **121**: 61–77.

Foster, S.P., Harrington, R., Devonshire, A.L., Denholm, I., Devine, G.J., Kenward, M.G., *et al.* 1996. Comparative survival of insecticide-susceptible and resistant peach-potato aphids, *Myzus persicae* (Sulzer) (hemiptera: aphididae), in low temperature field trials. *Bull. Entomol. Res.* **86**: 17–27.

Fournier, D. 2005. Mutations of acetylcholinesterase which confer insecticide resistance in insect populations. *Chem. Biol. Interact.* **157–158**: 257–261.

Garrison, E. & Marth, G. 2012. Haplotype-based variant detection from short-read sequencing. *arXiv* **1207.3907**.

Gautier, M., Foucaud, J., Gharbi, K., Cézard, T., Galan, M., Loiseau, A., *et al.* 2013. Estimation of population allele frequencies from next-generation sequencing data: pool versus individual-based genotyping. *Mol. Ecol.* **22**: 3766–3779.

Hivert, V., Leblois, R., Petit, E.J., Gautier, M. & Vitalis, R. 2018. Measuring genetic differentiation from pool-seq data. *Genetics* **210**: 315–330.

Hoffmann, A.A., Porter, S. & Kovacs, I. 1997. The response of the major crop and pasture pest, the red-legged earth mite (*Halotydeus destructor*) to pesticides: Dose-response curves and evidence for tolerance. *Exp. Appl. Acarol.* **21**: 151–162.

Hsu, J.C., Lin, Y.Y., Chang, C.C., Hua, K.H., May Chen, M.J., Huang, L.H., *et al.* 2016. Discovery of organophosphate resistance-related genes associated with well-known resistance mechanisms of *Plutella xylostella* (L.) (Lepidoptera: Plutellidae) by RNA-Seq. *J. Econ. Entomol.* **109**: 1378–1386.

Khajehali, J., van Leeuwen, T., Grispou, M., Morou, E., Alout, H., Weill, M., *et al.* 2010. Acetylcholinesterase point mutations in European strains of *Tetranychus urticae* (Acari: Tetranychidae) resistant to organophosphates. *Pest Manag. Sci.* **66**: 220–228.

Kuznetsova, A., Brockhoff, P.B. & Christensen, R.H.B. 2017. lmerTest package: tests in linear mixed effects models. *J. Stat. Softw.* **82**: 1–26.

Kwon, D.H., Cha, D.J., Kim, Y.H., Lee, S.W. & Lee, S.H. 2012a. Cloning of the acetylcholinesterase 1 gene and identification of point mutations putatively associated with carbofuran resistance in *Nilaparvata lugens*. *Pestic. Biochem. Physiol.* **103**: 94–100.

Kwon, D.H., Choi, J.Y., Je, Y.H. & Lee, S.H. 2012b. The overexpression of acetylcholinesterase compensates for the reduced catalytic activity caused by resistance-conferring mutations in *Tetranychus urticae*. *Insect Biochem. Mol. Biol.* **42**: 212–219. Elsevier Ltd.

Kwon, D.H., Clarkt, J.M. & Lee, S.H. 2010a. Extensive gene duplication of acetylcholinesterase associated with organophosphate resistance in the two-spotted spider mite. *Insect Mol. Biol.* **19**: 195–204.

Kwon, D.H., Im, J.S., Ahn, J.J., Lee, J.H., Marshall Clark, J. & Lee, S.H. 2010b. Acetylcholinesterase point mutations putatively associated with monocrotophos resistance in the two-spotted spider mite. *Pestic. Biochem. Physiol.* **96**: 36–42.

Langmead, B. & Salzberg, S.L. 2012. Fast gapped-read alignment with Bowtie 2. *Nat. Methods* **9**: 357–359.

Lawrence, M., Huber, W., Pages, H., Aboyoun, P., Carlson, M., Gentleman, R., *et al.* 2013. Software for computing and annotating genomic ranges. *PLOS Comput. Biol. Biol.* **9**: e1003118. Public Library of

Science San Francisco, USA.

Li, C.X., Kaufman, P.E., Xue, R. De, Zhao, M.H., Wang, G., Yan, T., *et al.* 2015. Relationship between insecticide resistance and kdr mutations in the dengue vector *Aedes aegypti* in Southern China. *Parasites and Vectors* **8**: 1–9. Parasites & Vectors.

Li, H. 2011. A statistical framework for SNP calling, mutation discovery, association mapping and population genetical parameter estimation from sequencing data. *Bioinformatics* **27**: 2987–2993. Oxford University Press.

Li, H., Handsaker, B., Wysoker, A., Fennell, T., Ruan, J., Homer, N., *et al.* 2009. The sequence alignment/map format and SAMtools. *Bioinformatics* **25**: 2078–2079.

Lynch, M. & Conery, J.S. 2000. The evolutionary fate and consequences of duplicate genes. *Science (80-.).* **290**: 1151–1155. American Association for the Advancement of Science.

Martinez-Torres, D., Devonshire, A.L. & Williamson, M.S. 1997. Molecular studies of knockdown resistance to pyrethroids: Cloning of domain II sodium channel gene sequences from insects. *Pestic. Sci.* **51**: 265–270.

Newman, L.J. 1925. The red legged earth mite *Penthaleus destructor* (Jack). *J. Dep. Agric. West. Aust.* **2**: 469–475.

Oakeshott, J.G., Devonshire, A.L., Claudianos, C., Sutherland, T.D., Horne, I., Campbell, P.M., *et al.* 2005. Comparing the organophosphorus and carbamate insecticide resistance mutations in cholin- and carboxyl-esterases. *Chem. Biol. Interact.* **157–158**: 269–275.

Pagès, H., Aboyoun, P., Gentleman, R. & DebRoy, S. 2017. Biostrings: Efficient manipulation of biological strings.

Paradis, E., Claude, J. & Strimmer, K. 2004. APE: analyses of phylogenetics and evolution in R language. *Bioinformatics* **20**: 289–290. Oxford University Press.

R Core Team. 2022. R: A language and environment for statistical computing (v4.1.3).

Ridsdill-Smith, T.J. 1997. Biology and control of *Halotydeus destructor* (Tucker) (Acarina: Penthaleidae): A review. *Exp. Appl. Acarol.* **21**: 195–224.

Riga, M., Bajda, S., Themistokleous, C., Papadaki, S., Palzewicz, M., Dermauw, W., *et al.* 2017. The relative contribution of target-site mutations in complex acaricide resistant phenotypes as assessed by marker assisted backcrossing in Tetranychus urticae. *Sci. Rep.* **7**: 1–12.

Robinson, M.T. & Hoffmann, A.A. 2000. Additional tests on the effects of pesticides on cryptic species of blue oat mite (*Penthaleus* spp.) and the redlegged earth mite (*Halotydeus destructor*). *Aust. J. Exp. Agric.* **40**: 671–678.

Roff, D.A. 1996. The evolution of threshold traits in animals. *Q. Rev. Biol.* **71**: 3–35.

Russell, R.J., Claudianos, C., Campbell, P.M., Horne, I., Sutherland, T.D. & Oakeshott, J.G. 2004. Two major classes of target site insensitivity mutations confer resistance to organophosphate and carbamate insecticides. *Pestic. Biochem. Physiol.* **79**: 84–93.

Shang, Q., Pan, Y., Fang, K., Xi, J., Wong, A., Brennan, J.A., *et al.* 2014. Extensive *Ace2* duplication and multiple mutations on *Ace1* and *Ace2* are related with high level of organophosphates resistance in *Aphis gossypii*. *Environ. Toxicol.* **29**: 526–533.

Thia, J.A., Hoffmann, A.A. & Umina, P.A. 2021. Empowering Australian insecticide resistance research with genetic information: the road ahead. *Austral Entomol.* **60**: 147–162.

Thia, J.A., Korhonen, P.K., Young, N.D., Gasser, R.B., Umina, P.A., Yang, Q., *et al.* 2022. The redlegged earth mite draft genome provides new insights into pesticide resistance evolution and demography in its invasive Australian range. *bioRxiv*, doi: 10.1101/2022.08.03.502713.

Umina, P.A. 2007. Pyrethroid resistance discovered in a major agricultural pest in southern Australia: the redlegged earth mite *Halotydeus destructor* (Acari: Penthaleidae). *Pest Manag. Sci.* **63**: 1185–1190.

Umina, P.A., McDonald, G., Maino, J., Edwards, O. & Hoffmann, A.A. 2019. Escalating insecticide resistance in Australian grain pests: contributing factors, industry trends and management opportunities. *Pest Manag. Sci.* **75**: 1494–1506.

Walsh, T.K., Joussen, N., Tian, K., Mcgaughran, A., Anderson, C.J., Qiu, X., *et al.* 2018. Multiple recombination events between two cytochrome P450 loci contribute to global pyrethroid resistance in *Helicoverpa armigera*. *PLoS One* **13**: e0197760.

Weir, B.S. & Cockerham, C.C. 1984. Estimating *F*-statistics for the analysis of population structure. *Evolution (N. Y).* **38**: 1358–1370.

Whitlock, M.C. 2019. OutFLANK: A procedure to find Fst outliers based on an inferred distribution of neutral Fst.

Yang, Q., Umina, P.A., Rašić, G., Bell, N., Fang, J., Lord, A., *et al.* 2020. Origin of resistance to pyrethroids in the redlegged earth mite (*Halotydeus destructor*) in Australia: repeated local evolution and migration. *Pest Manag. Sci.*, doi: 10.1002/ps.5538.

Yu, G., Smith, D.K., Zhu, H., Guan, Y. & Lam, T.T. 2017. ggtree: an R package for visualization and annotation of phylogenetic trees with their covariates and other associated data. *Methods Ecol. Evol.* **8**: 28–36. Wiley Online Library.

Zhang, L.J., Jing, Y.P., Li, X.H., Li, C.W., Bourguet, D. & Wu, G. 2015. Temperature-sensitive fitness cost of insecticide resistance in Chinese populations of the diamondback moth *Plutella xylostella*. *Mol. Ecol.* **24**: 1611–1627.